CHAPTER 2

Synthesis and mesomorphic properties of [S]-[+]-1-methylheptyl-4-[4'(3"-fluoro-4"-n-alkoxybenzoyloxy)benzoyloxy]-2-fluorobenzoates.

2.0 Introduction:

The presence or absence of a mesophase depends greatly on the chemical structure of the compound under investigation. Systematic studies have been carried out in order to establish empirical relationship between the chemical structure and thermal stabilities of various types of mesophases that a material may exhibit [1].

Soon after the discovery of ferroelectricity by Meyer *et* al. [2] in chiral Sm C* phase, its tremendous potential in the field of display technology was realized [3]. Since then, much attention has been devoted to the synthesis and study of chiral organic compounds with particular reference to ferroelectric properties.

In the year 1989, the discovery of antiferroelectric (Sm C^*_A) phase by Chandani *et* al. [4] in MHPOBC and the subsequent identification of tristable switching opened a new era in the field of display technology [5-11]. As a consequence, much research work has been carried out mainly concentrating on the synthesis of compounds exhibiting this phase and the suitability of such materials for applications [12-14]. Also considerable effort has been made to correlate the molecular structure of the compound to the appearance of the antiferroelectric phase [15] and certain empirical rules have been envisaged in this regard. However, the decisive factors that control the stability of this and other sub-phases are still unresolved. According to a recent review by Lagerwall [16], more than 1000 different compounds have been synthesized which show antiferroelectric behaviour. They often show a succession of phases from ferroelectric to antiferroelectric order, which are distinctly different and whose structures have not been fully understood to date.

The origin of antiferroelectricity has been attributed to the pairing of transverse dipole moment of the molecules in the adjacent layers [17]. The inherent stabilization of the antiferroelectric ordering seems to be produced by strong interaction ie.,

dipolar, quadrupolar and electrostatic interactions, between molecules in adjacent layers. Studies on the occurrence of antiferroelectric phase in relation to the molecular structure indicate that molecular chirality is one of the key factors that control the stability of this phase [18,22]. Relatively long molecular core lengths comprising a minimum of three aromatic rings and a chiral moiety close to it are found to give the highest chirality, which favour antiferroelectric smectic C^* phase.

2.0.1 Effect of extension of the molecular core length on the stabilization of the Sm C^*_A phase:

This effect can be illustrated by considering the following two compounds 2.1 [23,24] and 2.2 [25].

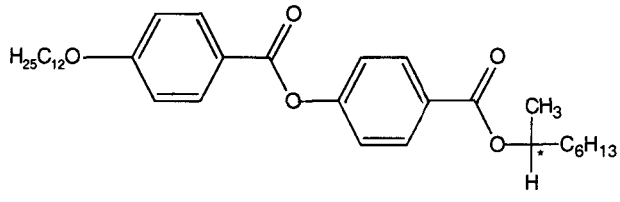

Cr 44.0 (Sm C* 22.0 Sm **A** 24.8) I

(2.1)

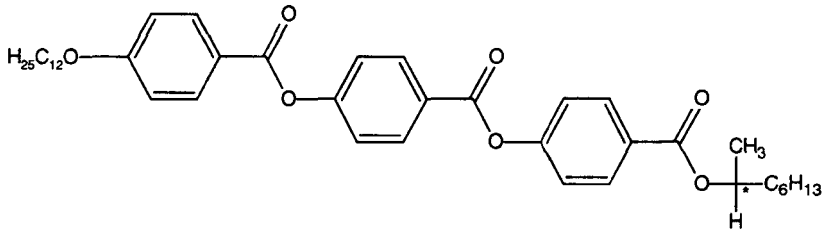

Cr 72.0 Sm C^*_A 85.6 Sm C^*_{F11} 87.5 Sm C^*_{F12} 92.3 Sm C^* 119.2 Sm A 131.5 I

(2.2)

From the transition temperatures mentioned above it is seen that compound 2.1 exhibits monotropic Sm C* and Sm **A** phases. In compound 2.2, where the molecular core length has been extended along the long molecular axis by the introduction of another phenyi ring, antiferroelectric and ferrielectric phases are induced and all the mesophases exhibited by this compound are enantiotropic. Thus, in compound 2.2,

there is an extension of conjugation along the long axis of the molecule, which favours the formation and stabilization of the ferro- and antiferroelectric phases.

Comparing the transition temperatures of compounds 2.3 [26] and 2.4 [27] we can draw similar conclusions. It can be seen that, compound 2.3 shows monotropic Sm C^*_A and Sm C^*, phases and the thermal range of the Sm C* phase is about 6.3°C. However, the addition of another benzoyloxy unit to 2.3 has resulted in a thermally more stable compound (2.4) having Sm C* and Sm C^*_A phases with a temperature range of ≈15°C and ≈43°C respectively. In addition to this, Sm C^*_α phase is induced between Sm **A** and Sm C* phases. All the mesophases exhibited by compound 2.4 are enantiotropic.

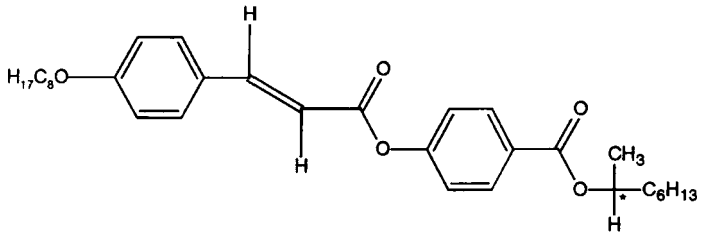

Cr 40.1 (Sm C^*_A 30.9 Sm C^*, 33.4) Sm C* 46.4 Sm A 57.8 I

(2.3)

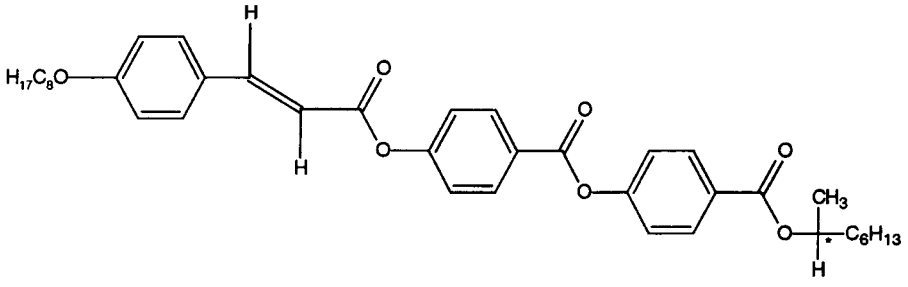

Cr 79.5 Sm C^*_A 124.0 Sm C^*_γ 126.0 Sm C^* 140.0 Sm C^*_α 142.0 Sm A 168.5 I

(2.4)

2.0.2 **Effect of the type of chiral moiety on the stability of the Sm C^*_A phase:**

Apart from the length of the molecular core, the stability of the Sm C^*_A phase is found to depend on the type and position of chiral moiety present in the material. Investigations regarding this have shown that the Sm C^*_A phase generally occurs in

compounds containing optically active octan-2-ol, 2-methyloctanoic acid, 1,1,1-trifluorooctan-2-01 *etc.*, [4,28-30] as the chiral moiety, where the chiral center is relatively close to the central rigid core of the molecule. In addition, increasing the length of the peripheral aliphatic chain on the other side of the chiral carbon upto seven carbon atoms results in the stabilization of the Sm C^*_A phase, after which it becomes destabilized [31]. The effect of chiral moiety on the occurrence and stability of the Sm C^*_A phase is illustrated in the following examples:

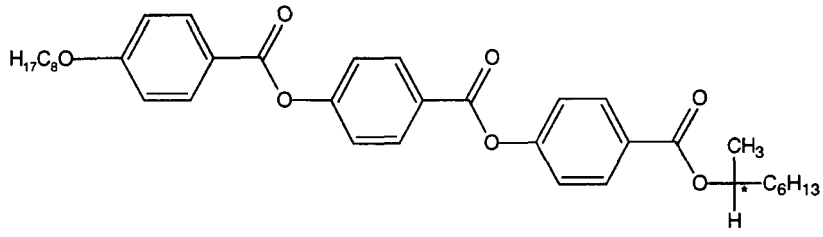

Cr 89.5 (Sm C^*_A 58.4 Sm C^*_{F11} 74.5 Sm C^*_{F12} 87.8) Sm C^* 90.8 Sm C^*_α 94.4 Sm A 139.7 I

(2.5)

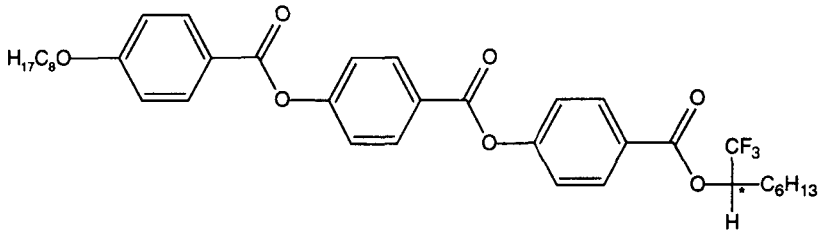

Cr 83.6 Sm C^*_A 100.3 Sm A 123.2 I

(2.6)

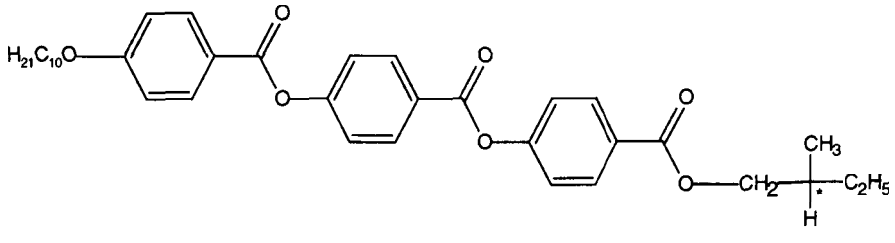

Cr 84.5 Sm C^* 127.5 Sm A 173.5 I

(2.7)

A comparison between compounds ***2.5*** [25], ***2.6*** [17] and **2.7** [32] shows that Sm C^*_A phase is favoured when optically active octan-2-ol or 1,1,1-trifluorooctan-2-ol is

used to prepare the chiral compound. The Sm C^*_A phase which is monotropic in compound 2.5 becomes enantiotropic on replacing the methyl group at the chiral center by trifluoromethyl group (compound **2.6**); however, Sm **C*** and other sub-phases present in 2.5 have completely disappeared in **2.6.** It is also seen that optically active 2-methylbutyl group present in **2.7** is not a favourable chiral moiety for inducing Sm C^*_A phase.

2.0.3 Effect of lateral fluoro substitution on the occurrence of different mesophases:

The type of mesophase exhibited by a liquid crystalline material depends largely on the intermolecular association of its constituent molecules. Hence, by appropriate modification of these interactions one can achieve selectivity in the types of mesophases exhibited by the compound. One way of modifying intermolecular associations of a given compound is by introducing substituents at the lateral positions in the core of the molecule. Such lateral substitution can bring about the following three effects:

(a) Depression in the melting (not always) and clearing temperatures
(b) Decrease in the length to breadth ratio of the molecule
(c) A change in the dipolar interactions.

Therefore stabilization or destabilization of a mesophase due to lateral substitution is governed by the effect that is more dominant (b or c). By and large fluorine is considered to be the most suitable lateral substituent for two reasons:

(a) The van der Waals radius of fluorine (≈1.47Å) is comparable to that of hydrogen (1.20Å); hence there is a very minimal decrease in the length to breadth ratio due to the fluoro substituent.
(b) Fluorine has a fairly large dipole moment.

In general, it is well known that strong lateral dipolar interactions between the constituent molecules favours the formation of smectic phases. Studies on the effect of lateral fluoro substituent on the stability of the mesophases have shown that lateral fluorine substitution at appropriate positions increase the smectic phase stability [34,35]. In addition to this, a lateral fluoro substituent tends to increase the lateral dipole moment, which in turn can induce molecular tilting and hence favour the

formation of tilted smectic phases. Prior to the discovery of antiferroelectricity, considerable effort was made to synthesize lateral fluoro substituted ferroelectric materials for display purposes. However, in the later years attention was turned towards synthesizing materials that exhibit the antiferroelectric phase. Investigations have shown that lateral fluoro substitution at some specific positions on the molecular core can bring about significant improvement in the temperature range of the antiferroelectric phase. The effect of lateral fluoro substitution on the stability and thermal range of ferroelectric, antiferroelectric and other sub-phases can be illustrated as follows:

Consider the following four compounds:

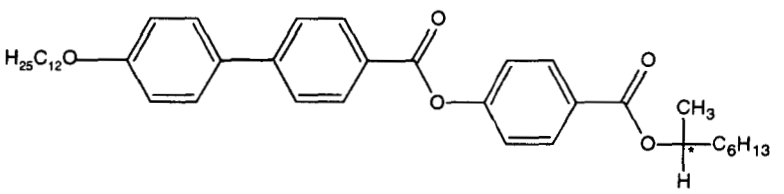

Cr 72.9 Sm C^*_A 99.9 Sm C^*_γ 103.5 Sm C^* 117.0 Sm C^*_α 122.2 Sm A 132.7 I

(2.8)

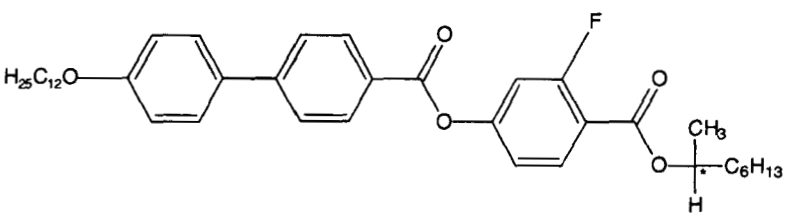

Cr 39.6 Sm C^*_A 108.4 Sm C^* 118.6 Sm A 126.7 I

(2.9)

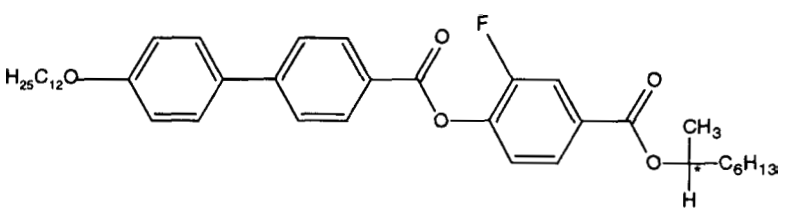

Cr 53.5 Sm C^*_A 78.3 Sm C^*_γ 82.0 Sm C^* 90.7 Sm A 105.7 I

(2.10)

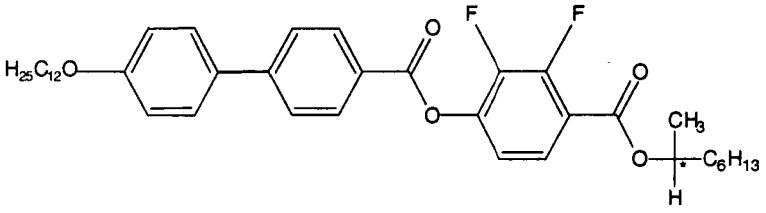

Cr 52.8 Sm C^*_A 94.0 Sm C^*_γ 95.2 Sm C^* 99.5 Sm A 110.8 I

(2.11)

From the transition temperatures of the above compounds it is evident that the unsubstituted parent compound **2.8** [33] has moderately high melting point and exhibits rich polymesomorphism consisting of an interesting range of tilted smectic phases below the Sm **A** phase. Compound **2.9** [34] which has a fluoro substituent *ortho* to the carboxylate group carrying the chiral center shows Sm C* and Sm C^*_A phases with an enhanced thermal range and a Sm **A** phase with a slightly reduced range of temperature. This can be attributed to the subtle polar and steric interactions between the neighbouring molecules containing a fluoro substituent. In addition to this, compound **2.9** shows a dramatic reduction in the melting point. In compound **2.10** [35] where the fluoro substitution is towards the center of the molecular core, the thermal range of Sm C^*_A phase is not affected significantly but there is a reduction in the mesophase transition temperatures including the melting and clearing temperatures by about 20 to25°C as compared to compound **2.8.** In compound **2.11** [34] where there are two fluoro substituents, one *ortho* to the caboxylate group and the other at *meta* position, the thermal range of Sm C^*_A phase is enhanced as compared to that of compound **2.10.** From the above comparison it is evident that a lateral fluoro substituent at the end of the core and close to the chiral center favours antiferroelectric phase with a fairly wide thermal range.

With a view to study the relationship between molecular structure and the occurrence of Sm C^*_A phase, we synthesized the following homologous series of compounds **(2.12)** containing a fluoro substituent in two different positions.

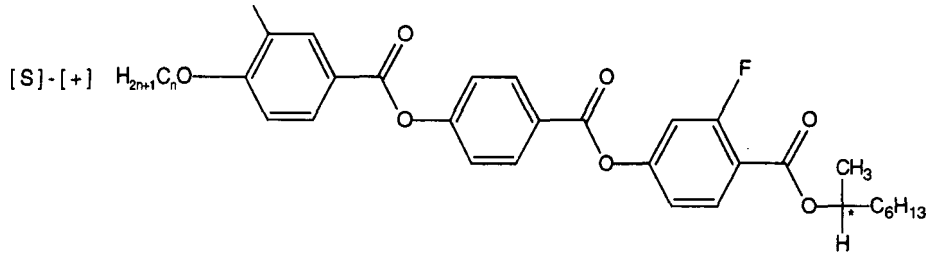

n = 7,8,9,10,11,12,14,16,18.

(2.12)

2.1 **Results and discussion:**

The synthesis of compounds belonging to series 2.12 was carried out as outlined in a scheme shown in figure **2.1.**

The 3-fluoro-4-n-alkoxybenzoic acids were prepared following the procedure described by Gray and Jones [36]. **2-Fluoro-4-benzyloxybenzoic** acid (2.28, **section** 2.3) was prepared by first reacting ethyl 2-fluoro-4-hydroxybenzoate with benzyl chloride in the presence of anhydrous potassium carbonate in butan-2-one followed by hydrolysis of the resulting ester with aqueous alkali. [S]-[+]-1-Methylheptyl-2-fluoro-4-benzyloxybenzoate (2.29) was obtained by a esterification reaction of 2.28 with [S]-[+]-2-octanol in the presence of 1,3-dicyclohexylcarbodiimide (DCC) as a dehydrating agent and 4-N,N'-dimethylaminopyridine (DMAP) as a catalyst. Deprotection of the phenolic group through a palladium catalyzed hydrogenolysis reaction yielded [S]-[+]-1-methylheptyl-2-fluoro-4-hydroxybenzoate (2.31). [S]-[+]-1-Methylheptyl-4-(4'-hydroxybenzoyloxy)-2-fluorobenzoate (2.35) was obtained by a similar sequence of reactions. Hydrogenolysis was performed in ethylacetate using 5% Pd-C as catalyst at room temperature. The final esters were obtained by carrying out esterification reaction of 2.35 with the appropriate 3-fluoro-4-n-alkoxybenzoic acids, at room temperature using dichloromethane as the solvent.

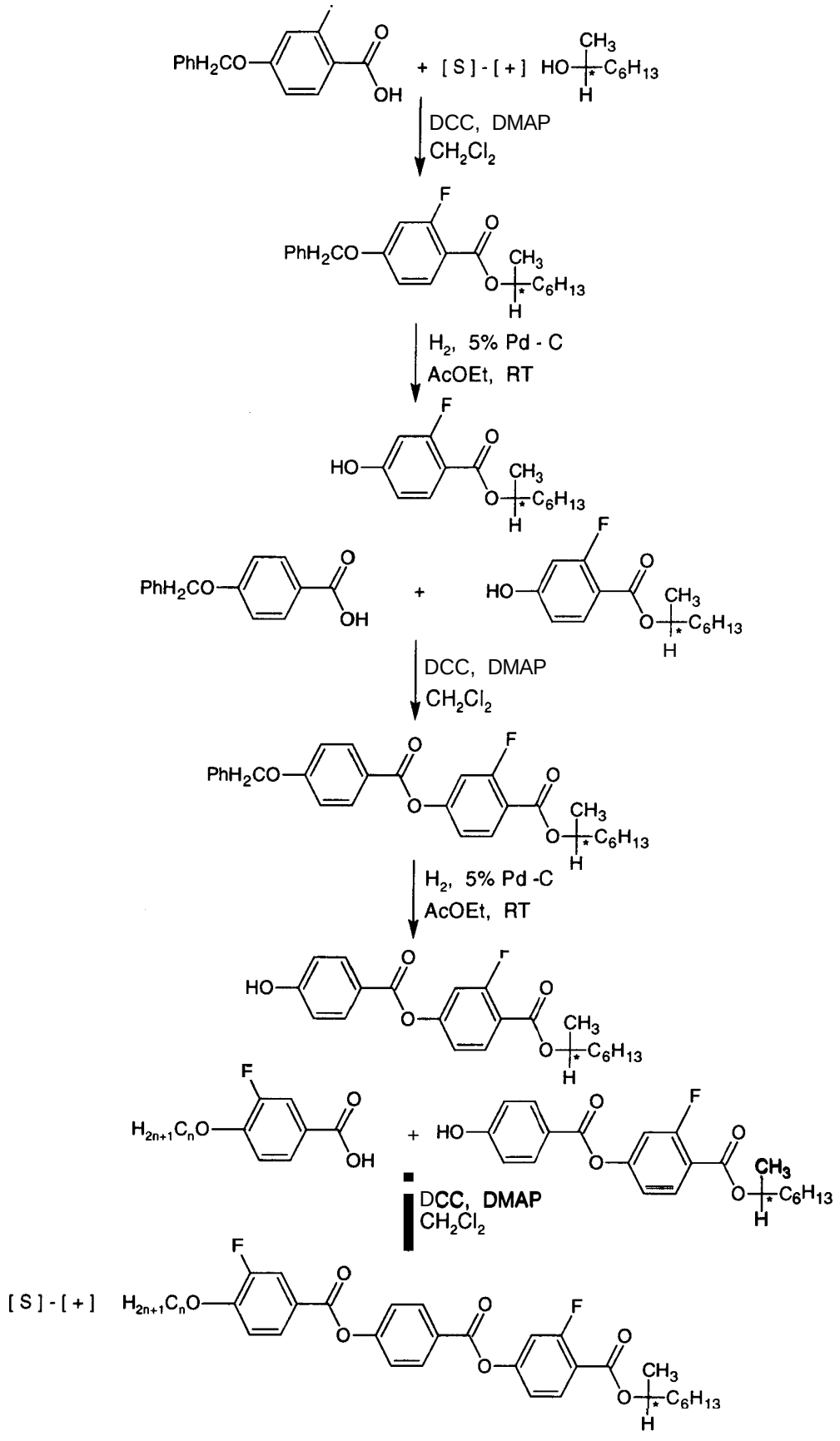

n = 7,8,9,10,11,12,14,16,18.

Fig 2.1 : Synthetic scheme for preparation of compounds of series 2.12.

As a preliminary investigation, the mesophases exhibited by these compounds were examined using an optical polarizing microscope. Thin films of the samples were obtained by sandwiching them between a glass slide and a cover slip. All the compounds in this series show rich polymesomorphism. On cooling the isotropic liquid in an ordinary slide, both homeotropic as well as focal-conic textures characteristic of the Sm A phase was observed. On further cooling, fine bands appeared on the existing focal-conic texture (banded focal-conic). This texture was similar to the one observed for the Sm C^* phase. On decreasing the temperature further (for compounds 1 to 7) the bands became highly coloured and broader and the resultant texture was similar to that observed for the Sm C^*_A phase.

In order to establish the identity of the mesophases, the samples were examined on different cells coated for both homogeneous and homeotropic alignments. For a homogeneous alignment, the cells were coated with polyimide and rubbed in a direction parallel to the length of the glass plates. When the isotropic liquid of compound 4 was cooled on such a cell, homogeneous coloured regions with some focal defects typical of the Sm A phase [37] was observed and a photomicrograph of this is shown in plate 2.1.

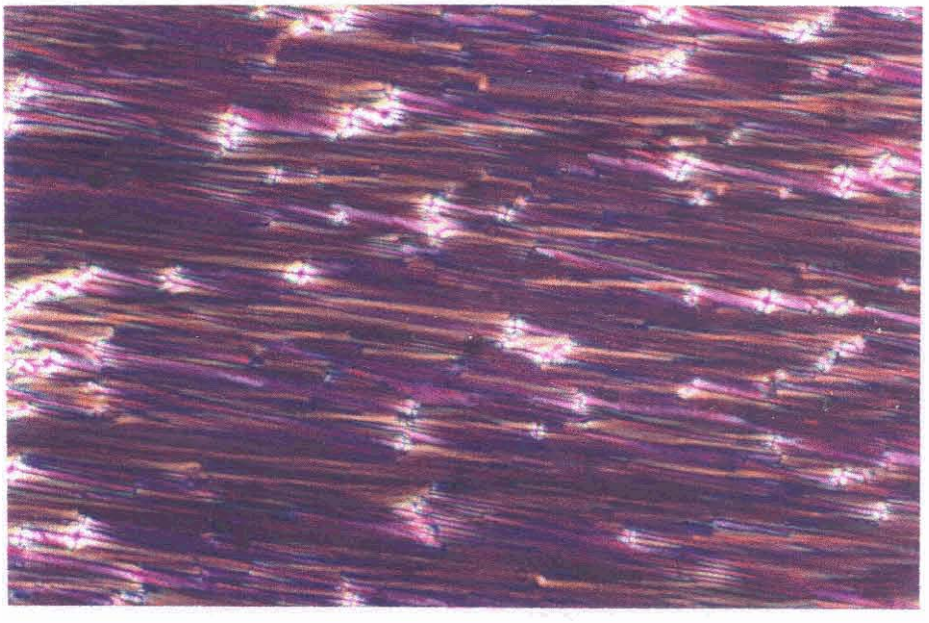

Plate 2.1 : Photomicrograph of compound 4 showing Sm A phase(homogeneously aligned) at 127°C.

When the temperature was gradually decreased, the existing texture became striated with bright bands which grew parallel to the rubbing direction as shown in plate 2.2. This type of texture has been observed for Sm C^*_α [37] phase appearing below the Sm A phase.

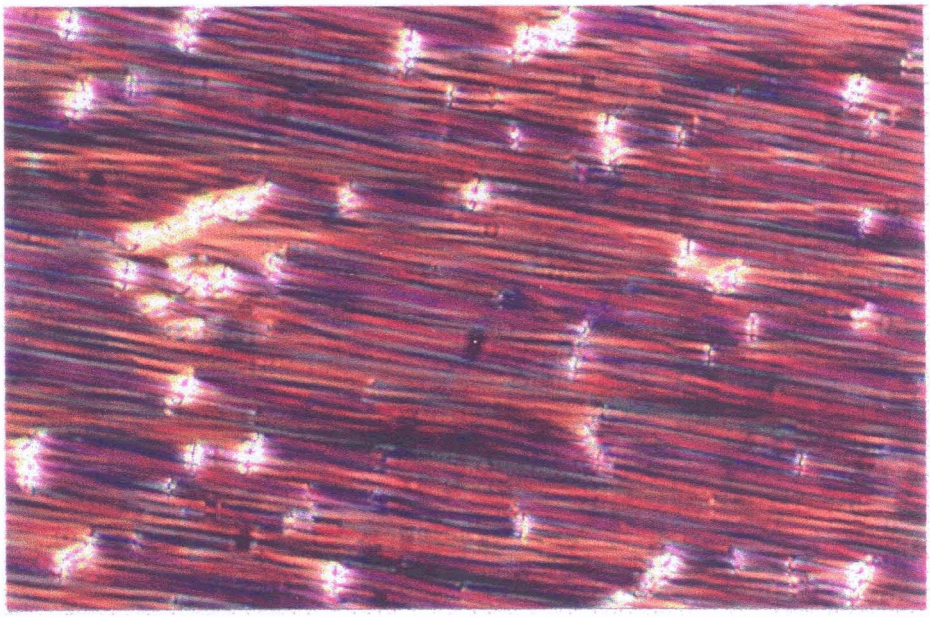

Plate 22 : Photomicrograph of compound 4 showing Sm C^*_α phase (homogeneously aligned) at 120.6°C.

On further cooling the sample, rope-like texture characteristic of the Sm C* phase [37] was observed. A typical photomicrograph of this texture is shown in plate 2.3.

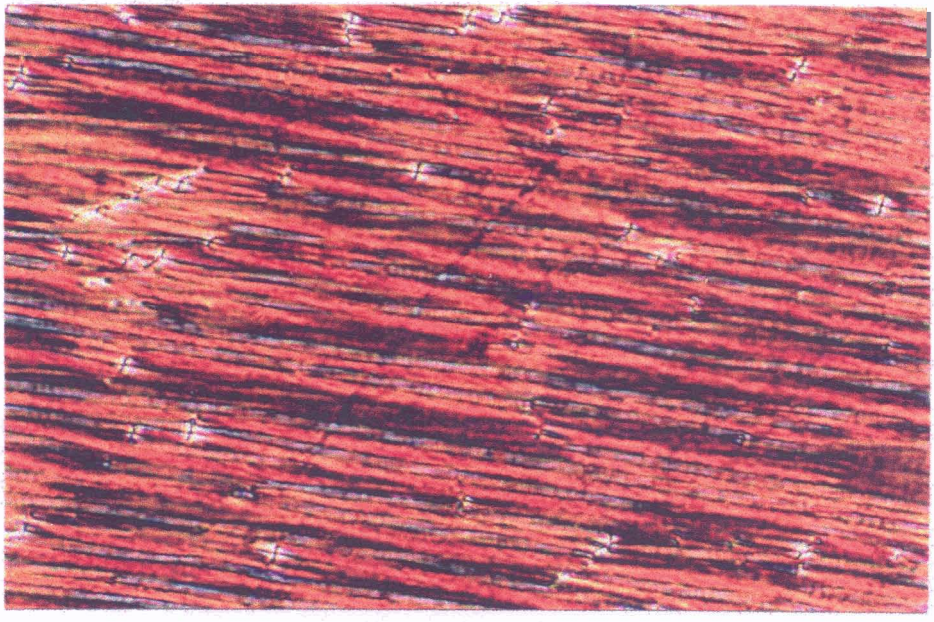

Plate 23 : Photomicrograph of compound 4 showing Sm C^* phase (homogeneously aligned) at 118.7°C.

On cooling this phase, stripes start growing in a direction perpendicular to the rubbing direction on the rope-like texture as shown in plate 2.4. This texture was identical to the pattern observed for the Sm C^*_A phase [37].

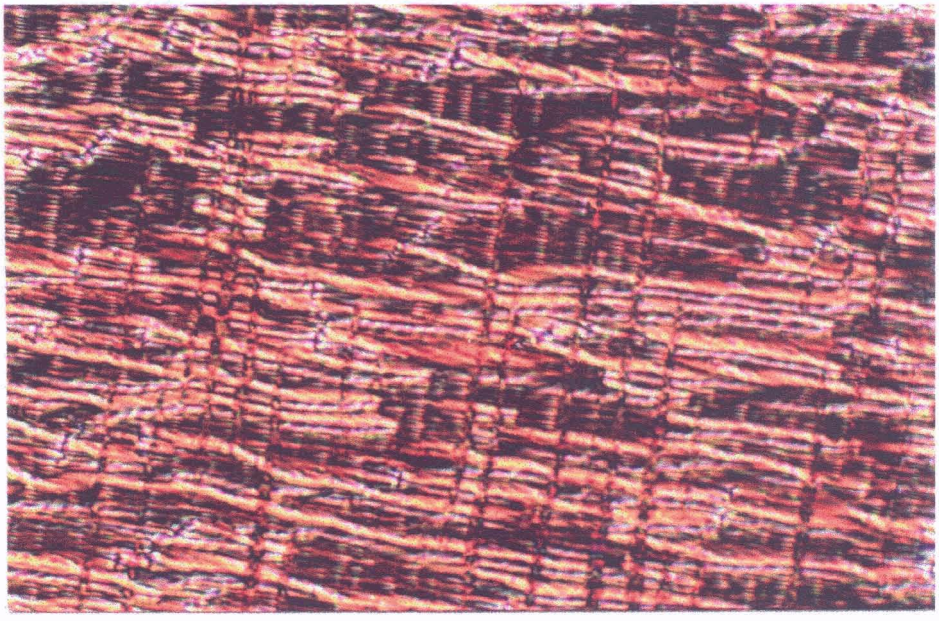

Plate 2.4 : Photomicrograph of compound 4 showing Sm C^*_A phase (homogeneously aligned) at 111°C.

On cooling the isotropic liquid of compound 2 in a homeotropically aligned cell, below the Sm C* phase, a birefringent, non-iridescent plane texture was observed as shown in plate 2.5. The characteristic feature of this phase in this alignment is that the texture appeared to be in constant motion eventhough the temperature is held constant. This type of texture has been observed for Sm C^*_γ phase [38] and we observed the same for compounds 2, 3, 5 and 7.

Therefore from these textural observations, we have been able to identify that compounds of series 2.12 exhibit Sm A, Sm C^*_α, Sm c*, Sm C^*_γ and Sm C^*_A phases.

In order to conclusively establish the identity of the different smectic phases exhibited by these compounds a miscibility study of the n-nonyloxy homologue (compound 3) with the well-known standard material 1-methylheptyl-4-(4'-n-octadecyloxybiphenylcarbonoyloxy)benzoate (MHPOBC) [4] which exhibits the above mesophases, was carried out and an isobaric binary phase diagram constructed is shown in figure 2.2.

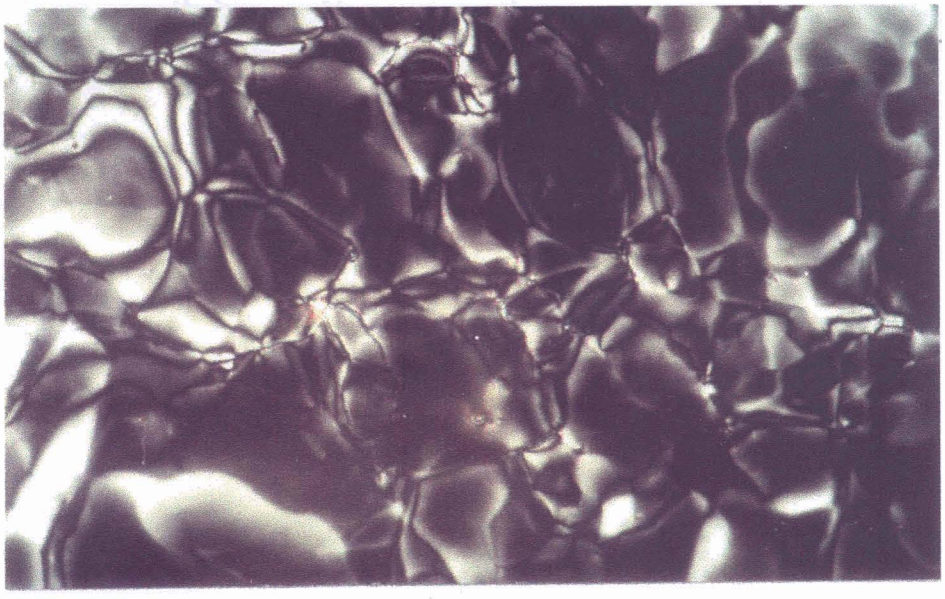

Plate 2.5 : Photomicrograph of compound 2 showing Sm C^*_γ phase (homeotropically aligned) at 116.7°C.

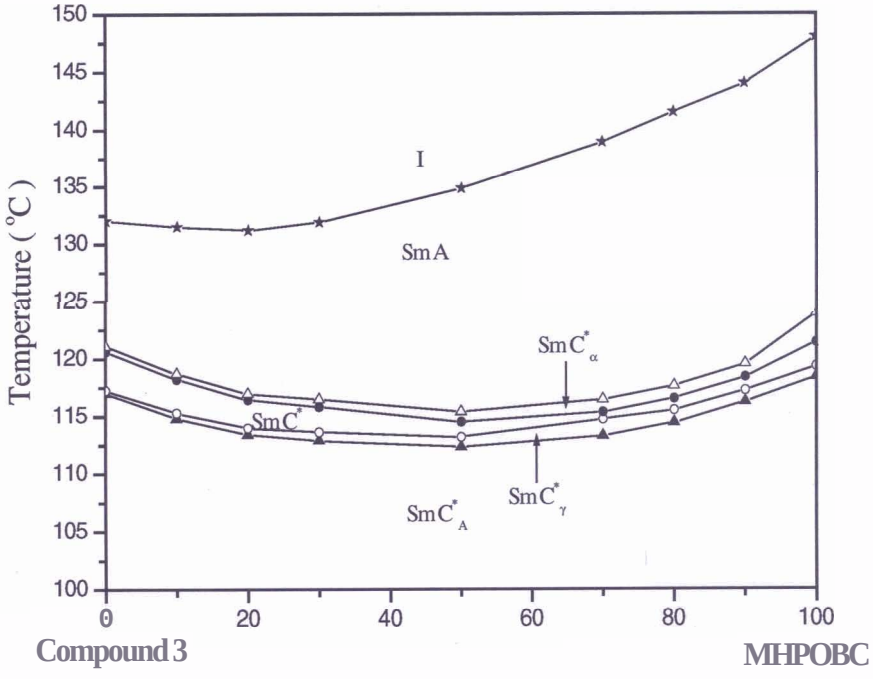

Fig 2.2 : Miscibility phase diagram of binary mixtures of compound 3 and the standard material MHPOBC.

The mixtures were prepared as weight/weight ratio and mixed well in their isotropic states. In this diagram a complete miscibility of all the phases over the entire composition range can be seen.

The transition temperatures along with the associated enthalpies obtained from the DSC thermograms are summarized in table 2.1.

From this, table it is seen that Sm A and Sm C^*_α phases precede the other helical smectics over the entire series. The temperature range of the Sm C^*_α phase is rather narrow and is between 0.2 to 0.5°C. The Sm C^* phase exists in all the compounds and is more dominant for compounds 8 and 9 (table 2.1) where the temperature range is about 50-60°C. The Sm C^*_A phase appears from compound 1 up to compound 7. In this series compound 6 has the highest temperature range of antiferroelectric phase (50.2°C). In some of the compounds of this series the Sm C* and Sm C^*_A phases are separated by the intermediate Sm C^*_γ phase, which exists over a short thermal range of 0.5-1°C. All the compounds of this series exhibit, Sm A, Sm C^*_α and Sm C^* phases while only seven compounds show the Sm C^*_A phase. Compounds 8 and 9 do not exhibit the Sm C^*_A phase. The ferrielectric phase was observed in only four compounds.

Table 21 : Transition temperatures (°C) and enthalpies (kJ mol^{-1}) for [S]-[+]-1-methylheptyl-4-[4'-(3"-fluoro-4"-n-alkoxybenzoyloxy)benzoyloxy]-2-fluorobenzoates.

Compound number	n	Cr	Sm C^*_A	Sm C^*_2	Sm C^*_3	Sm A	I
1	7	63.0 *20.8*	112.5 *0.04*		113.0 †	114.0 *0.03*	139.0 *5.32*
2	8	69.5 *21.8*	116.5 †	117.0 †	117.5 †	118.5 †	135.5 *5.23*
3	9	93.5 *29.3*	117.0 *0.02*	117.5 *0.04*	120.5 †	121.0 †	132.0 *5.02*
4	10	101.0 ⊗*31.9*	118.0 *0.07*		122.5 †	123.0 *0.33*	130.5 *4.68*
5	11	90.0 *27.9*	112.5 *0.01*	113.0 *0.05*	122.0 †	122.5 †	129.0 *5.05*
6	12	60.5 ⊗*27.7*	111.0 *0.05*		121.0 †	122.0 †	127.5 *4.91*
7	14	57.0 ⊗*39.5*	98.0 †	99.5 *0.04*	119.5 †	120.0 †	124.5 *4.92*
8	16	62.0 ⊗*34.7*			115.5 †	116.5 *0.42*	121.5 *4.89*
9	18	52.0 *34.8*			112.0 †	112.5 †	118.0 *4.62*

† : The enthalpy could not be measured; ⊗ : Total enthalpy including any other crystal-crystal transition.

A plot of the number of carbon atoms in the n-alkoxy chain ***versus*** the transition temperatures of homologous series 2.12 is shown in figure 2.3.

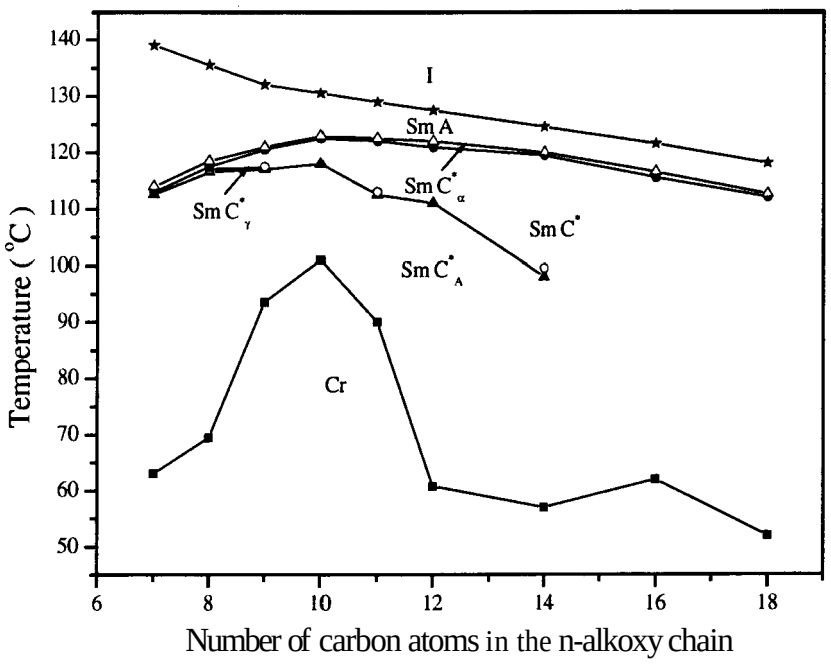

Fig 2.3 : A plot of transition temperatures *versus* the number of carbon atoms in the n-alkoxy chain.

The plot shows smooth curve relationship for like transitions. It can be seen that the clearing temperatures decrease with increase in the chain length. For the Sm A to Sm C^*, transition, there is a gradual increase in the transition temperature up to compound 4 after which it shows a decreasing trend with the increase in the alkoxy chain length. A similar trend is also seen for the Sm C^*_α-Sm C* and Sm C^*- Sm C^*_A transitions. The Sm C^*_γ-Sm C* transition temperature increases initially on moving from compound 2 to compound 3, followed by a decrease with a further increase in the chain length (compounds 5 and 7).

As a proof for the existence of chiral phases, [R]-[-]-enantiomer of compound 2 was prepared and a contact preparation between this and the [S]-[+] enantiomer was made. **A** photomicrograph of the contact preparation is shown in plate 2.6. The phase sequence exhibited by the racemate was different when compared to that of the pure

enantiomers. In this case the I↔Sm A↔Sm C^*_α↔Sm C^*↔Sm C^*_γ↔Sm C^*_A was replaced by I↔Sm A↔Sm C ie., all the chiral smectic phases disappear in the racemic mixture. From plate 2.6 it can be seen that on either side of the region of contact, banded focal-conic texture is visible which is characteristic of the Sm C* phase, while at the region of contact where the two helices are compensated (racemic), a schleiren texture characteristic of the achiral Sm C phase is formed.

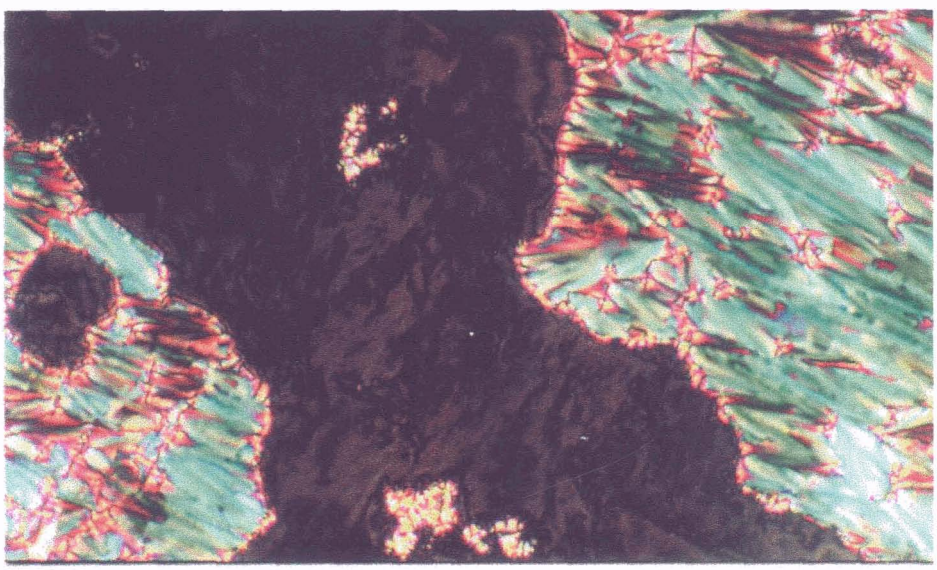

Plate 2.6 : Photomicrograph of a contact preparation between the [S]-[+] and [R]-[-] enantiomem of 1-methylheptyl-4-[4'-(3"-fluoro-4"-n-octyloxybenzoyloxy) benzoyloxy]-2-fluorobenzoate at 115°C. At this temperature both the enantiomem are in their Sm C* phase; at the region of contact the pitch gets compensated resulting in a Sm C phase.

Figure 2.4 shows the DSC thermogram of compound 2. The sample was heated and cooled at rates of 5°C and 3°C/min. At the slower rate, the Sm C^*_A↔Sm C^*_γ↔Sm C^*↔Sm C^*_α transitions could be clearly seen. The ^{1}H NMR spectrum of compound 9 is shown in figure 2.5.

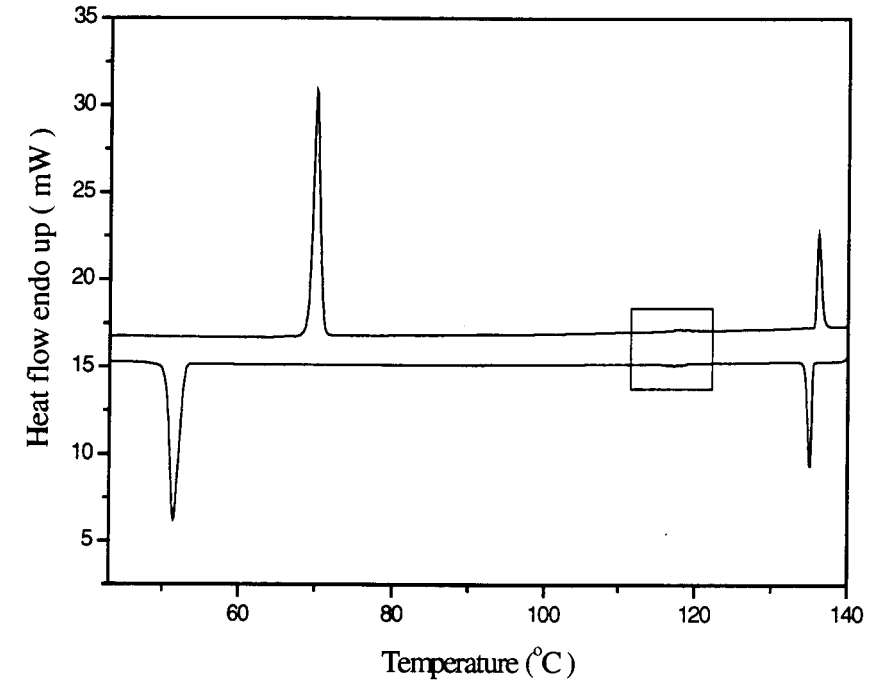

(a)

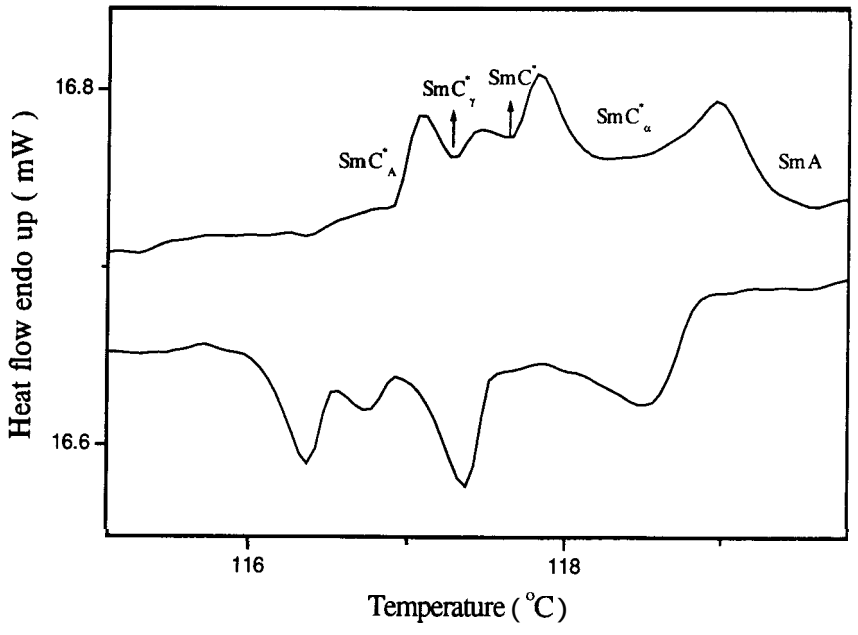

(b)

Fig 2.4 : DSC thermogram of compound 2 (series 2.12). (a) Scan at 5°C/min.; (b) The enlarged view of the box shown in fig 2.4a; Scan at 3°C/min., where the Sm $C^*_A \leftrightarrow$ Sm $C^*_\gamma \leftrightarrow$ Sm $C^* \leftrightarrow$ Sm C^*_α transitions are well resolved.

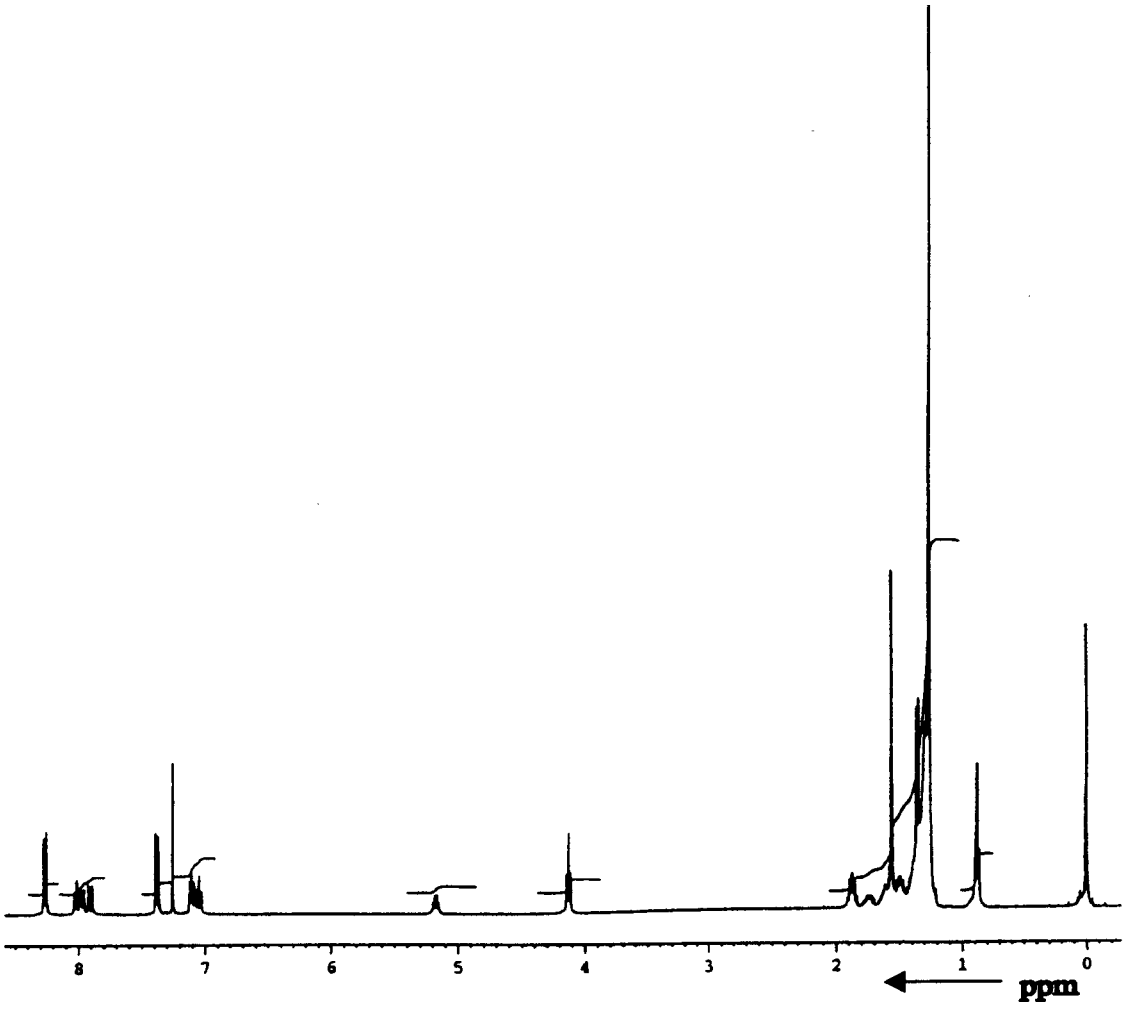

Fig 2.5 : ^{1}H NMR spectrum of compound 9 (series 2.12).

Faye ***et*** al. [25] have synthesized the following four homologous series of compounds and have studied the effect of the position of fluoro substituent on the stability of the Sm C^{*}_{A} and other sub phases.

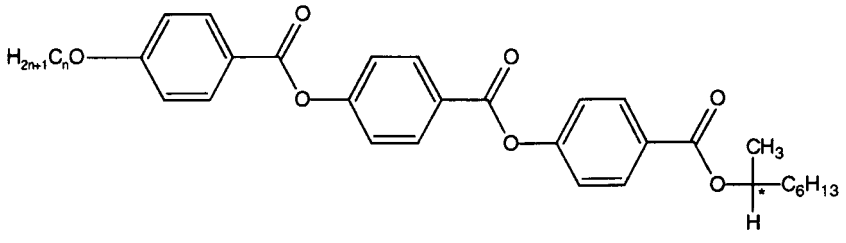

n = 7,8,9,10,11,12.

(2.13)

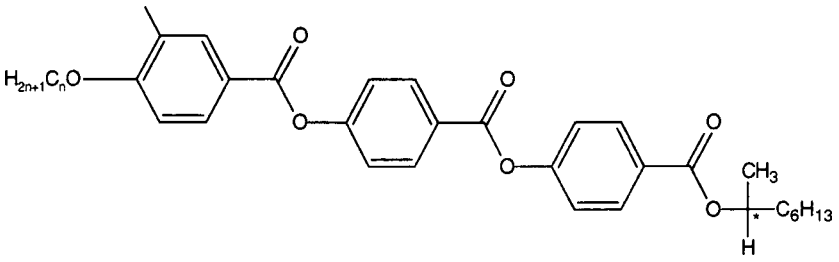

n = 8,9,10,11,12.

(2.14)

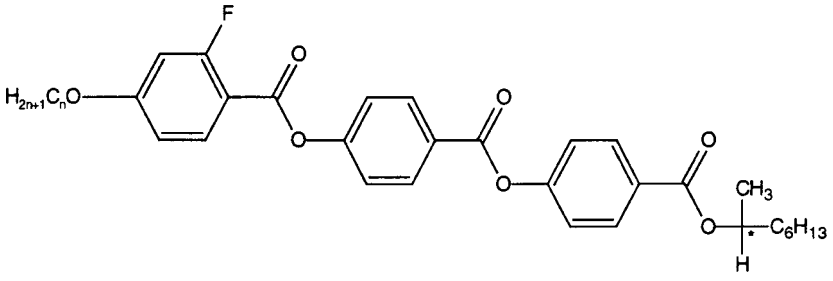

n = 8,9,10,11,12.

(2.15)

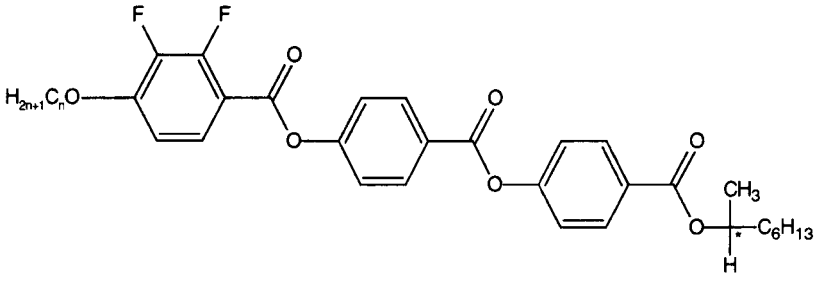

n = 8,9,10,11,12.

(2.16)

The results of their investigations are summarized below [25]:

In series **2.13,** homologues n = 8 to 10 exhibit Sm C^*_A, Sm C^*_{F11}, Sm C^*_{F12} (F_{11} and F_{12} are two types of isostructural helicoidal femelectric phases), Sm C^*, Sm C^*_α and Sm A phases. The higher homologues n = 11 and 12 exhibit all the above phases

except for the Sm C^*_α phase and in n = 7, the Sm C^*_A, Sm C^*_{F11} and Sm C^*_{F12} phases are absent. In series 2.14, homologues n = 9 to 12 exhibit Sm C^*_A, Sm C^*_{F11}, Sm C* and Sm **A** phases and n = 8 to 10 showed Sm C^*_α phase in addition to the above phases. None of the homologues of this series showed Sm C^*_{F12} phase. In series 2.15, the homologues n = 9 to 11 showed Sm c*, Sm C^*_α and Sm **A** phases. The highest homologue n = 12, exhibited a monotropic Sm C^*_A and an enantiotropic Sm C^*_{F11} phases in addition to the above phase sequence. The homologue n = 8 showed only a Sm A phase. Homologues n = 9 to 12 of series 2.16 exhibit Sm C^*_A, Sm C^*_{F11}, Sm c*, Sm C^*_α and Sm **A** phases. Homologues n = 9 to 11 showed a Sm C^*_{F12} phase in addition to the above phase sequence and n = 8 exhibited only Sm C^*_α and Sm A phases.

The three ring esters possess a strong longitudinal moment due to the three-carboxyl linkages [25]. In series 2.15 where there is a fluorine substitution towards the central molecular core, there is a considerable increase in the value of this moment, which leads to a stabilization of the Sm **A** and Sm C^*_α phases, and disappearance of the Sm C^*_A and Sm C^*, phases (in the lower homologues). The highest homologue n = 12 shows a monotropic Sm C^*_A phase and an enantiotropic Sm C^*_{F11} phases. On the contrary a fluoro substituent *ortho* to the alkoxy chain as in series 2.14, decreases the longitudinal moment and hence the whole range of mesophase sequence present in the parent series (2.13) exists. However the Sm C^*_A phase in this series is stabilized to some extent as compared to 2.13. In series 2.16 where there is a difluoro substitution, the net moment is increased slightly preserving the same mesophase sequence as observed in series 2.13.

From the above results and the discussion presented earlier, it is probable that the presence of fluoro substituents *ortho* to the carboxylate group close to the chiral center (2.9) and to the terminal alkoxy chain (2.14) favour not only the formation but stabilizes the Sm C^*_A phase. By incorporating such substitutions in a single compound we have been able to achieve a sufficiently long thermal range of Sm C^*_A phase.

The mesomorphic behaviour of series 2.12 can be compared with those of series 2.13. In series 2.12, due to the presence of lateral fluoro substituents closer to both the chiral center and the terminal alkoxy chain, the melting and clearing temperatures have been lowered. As far as the Sm C^*_A phase is concerned, in series 2.13 this phase does not exist for the homologue n = 7 and for homologues n = 8 and 9 it is monotropic and for the higher homologues it is enantiotropic with a short thermal range. However, in series 2.12 there is a large increase in the thermal range of the Sm C^*_A phase with compound **3** having a thermal range of 50.2°C. For sufficiently long chain lengths (n = 16 and 18) the Sm C^*_A phase disappears and Sm **C*** phase with a wide thermal range of 40-50°C predominates. Enantiotropic Sm C^*_α phase appears in all the homologues of this series. The thermal range of Sm A phase is reduced when compared to series 2.13.

A similar comparison can be made between series 2.12, 2.14 and 2.15. By combining all the three series, the order in which the clearing temperatures decrease is **2.14>2.12>2.15**. Once again the thermal range of Sm C^*_A phase in series 2.12 is enhanced to a greater extent when compared to series 2.14 and 2.15. Infact in series 2.15, Sm C^*_A phase is absent in homologues n = 8 to 11 and exists as a monotropic phase in n = **12** (highest homologue).

Therefore these results show that the presence of lateral fluoro substituents *ortho* to the terminal alkoxy chain and to the carboxylate group close to the chiral center (2.12) influence the formation and stabilizes the Sm **C*** and Sm C^*_A phases. In conclusion, it can be said that

(a) Presence of a fluorine substituent *ortho* to the carboxylate group close to the chiral center

(i) increases the tranverse moment next to the chiral center.

(ii) restricts the rotation of the chiral moiety with respect to the long molecular axis, there by increasing the overall chirality of the molecule.

Both these factors favour the formation of Sm C^*_A.

(b) Presence of a lateral fluorine substituent *ortho* to the terminal alkoxy chain brings about a decrease in the longitudinal moment which favours the formation of the Sm C^*_A phase.

General methods of investigation:

All the solid intermediates and final compounds were purified by column chromatography on silica gel (60-120 mesh, ACME, India) using appropriate solvents (pure) or mixtures of solvents as eluent. Intermediates, which are liquids, were vacuum distilled. The purity of all the intermediates and final compounds were checked by thin layer chromatography using TLC aluminium cards coated with silica gel $60F_{254}$ with a fluorescent indicator manufactured by Merck, Germany. The spots on these plates were rendered visible by exposing them to a DESAGA HP-UVIS lamp at 254 and /or 366nm. Normal phase high performance liquid chromatography was performed on the final compounds using μ porasil column (3.9mmX300mm, Waters Associates Inc.) and 1% acetone in dichloromethane as the eluent. The chemical structure of all the compounds was confirmed by using a combination of infrared absorption spectroscopy (Shimadzu IR 435 spectrophotometer as nujol mull unless otherwise specified), nuclear magnetic resonance spectroscopy (AMX 400 spectrometer with tetramethylsilane as an internal standard) and mass spectroscopy (JEOL SX 102/DA-6000). The chemical shifts in NMR are quoted as "δ" (parts per million) downfield from the reference. $CDCl_3$ was used as the solvent for all the final esters. Specific optical rotations were measured on an Optical Activity AA 1000 polarimeter using chloroform/acetone/tetrahydrofuran (THF) as the solvent. The enthalpies and transition temperatures were determined from thermograms obtained on a Perkin-Elmer, Pyris 1 D differential scanning calorimeter. The calorimeter was calibrated using pure indium as a standard.

2.2 Spontaneous polarization (P_S):

Classically, this is a macroscopic property associated with ferroelectric and antiferroelectric liquid crystals. It is an extremely potent investigative tool in the elucidation of the physical properties and structures of chiral liquid crystals, yielding much information on the internal environment of the mesophase.

The origin of spontaneous polarization in ferroelectric and antiferroelectric liquid crystals has been discussed in detail in chapter 1. From the studies relating the polarization with the molecular structure, it can be concluded that P_S is primarily dependent on a coupling between the local dipoles at, or in the proximity of, the asymmetric centers of the molecules in the ferroelectric mesophase. The effect of core structure on the value of P_S depends on whether the direction of dipole in the vicinity of the chiral center is such that it adds up or opposes the dipole at the chiral center thereby increasing or decreasing the value of P_S [23].

The temperature dependence of the polarization generally follows a power law ie.,

$$P_S(T) = P_S^o (T - T^*)^\alpha,$$

where, P_S(T) is the polarization at temperature $T(^oC)$, P_S^o is a constant, T*is the X-C* phase transition temperature (X=Sm A or Sm c*,), and T is the temperature at which measurements are made. As a general rule the polarization in the Sm C* phase increases with an increase in the reduced temperature $(T - T^*)$ and finally gets saturated at low temperatures. However, there are a few exceptions to this behaviour [39,40] wherein, a slow increase in the value of P_S is observed in the vicinity of phase transition followed by a rapid rise in the value as the temperature is lowered.

2.2.1 Measurement of spontaneous polarization:

Several techniques have been employed for the measurement of spontaneous polarization of ferroelectric liquid crystals [41,42,43]. One of the standard classical methods is the Tower-Sawyer [44] technique. In this technique, a low frequency sine-wave a.c. field of sufficiently high amplitude is applied to the ferroelectric sample and a plot of the input versus output signals produces a hysterisis loop characteristic [45]

of a ferroelectric material. However the main drawback of this method is that even a small part of ionic and capacitive contribution can distort the hysterisis loop. Therefore for our measurements we have adopted the modified form of this method proposed by Diamant ***et al.*** [46] which overcomes the drawback of the Tower-Sawyer technique. In this method, also usually referred to as the hysterisis loop method, two parallel Tower-Sawyer circuits are used, one containing the sample and the other a resistor capacitor combination, both of which can be varied independently. The latter enables compensation of ionic and linear capacitive portions of the output signal, which is achieved by feeding the output from the sample and the compensating Tower-Sawyer circuit to a differential amplifier. In this method we applied a triangular low frequency a.c. field to switch the sample as this waveform has the unique advantage of separating the capacitive contribution from interfering with the current due to polarization reversal. Figure 2.6 represents a block diagram of the circuit employed for measuring the spontaneous polarization.

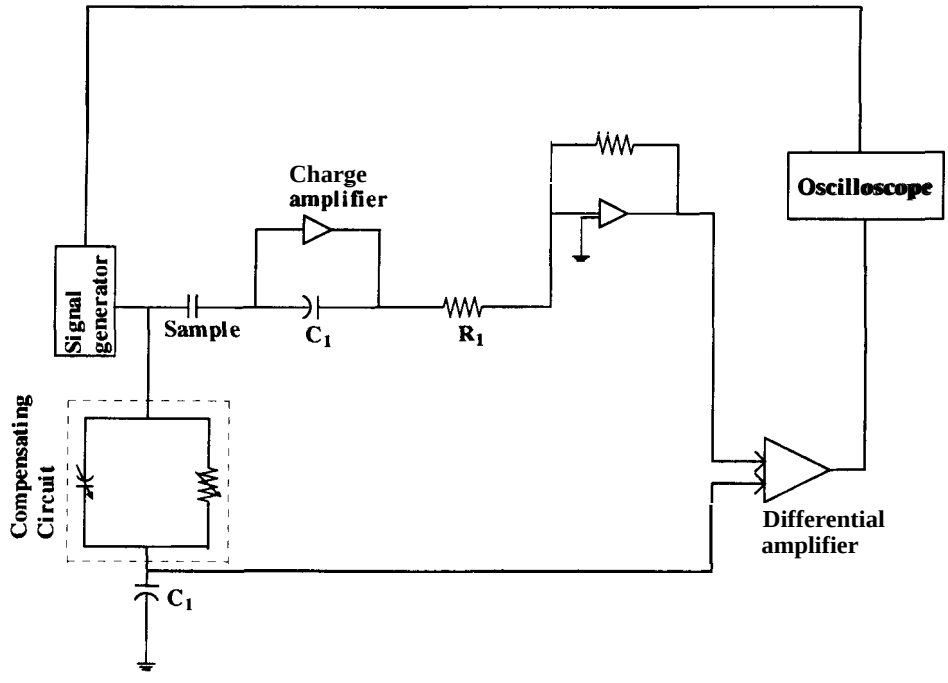

Fig 2.6 : Block diagram of the circuit employed for spontaneous polarization measurement.

Spontaneous polarization measurement was carried out using sample cells made up of two thin (thickness ≈0.8mm), flat, transparent glass plates, coated with indium tin

oxide (ITO) and etched appropriately to create an active area for accurate measurement. In order to obtain sample aligned in the homogeneous (planar) bookshelf geometry, the plates were treated with polyimide solution, cured at 300°C for an hour and finally were rubbed unidirectionally. The thickness of the cell was controlled by using mylar spacers. The two glass plates were joined together by a non-reactive glue and cured at 150°C. Before performing the polarization measurements, the active area and thickness of the cell were measured accurately. During the measurement of P_S, the sample was cooled at a slow rate (0.2°/min) from the isotropic phase under a triangular a.c. field of low frequency (20-25Hz) having an amplitude of $\approx$10-14V_{pp} to get good alignment. The experiment was performed under cooling mode. Throughout the measurement, the shape of the hysterisis loop was monitored using a dual channel storage oscilloscope (Aplab 3660D) and any contribution to the output signal due to the ionic impurities which distorts the shape of the loop was nullified by manually adjusting the values of the variable capacitor and resistor in the compensating circuit.

2.2.2 Results:

The temperature dependence of spontaneous polarization was determined and plots of P_S versus reduced temperature (T-T*) were obtained for six homologues of the series **2.12** (n=10,11,12,16,18). Figures 2.7-2.9 represent these plots. From the plots it is seen that they follow a general pattern and for all compounds P_S is found to decrease with the increase in temperature and the value lies close to zero at T* (T* is the Sm C^*_α-Sm C* transition temperature). The most interesting feature is that, a decrease in the magnitude of polarization is observed with the increase in the chain length. Figure 2.10 shows a plot of P_S at $T-T^* = -4$°C as a function of chain length. From the plot it can be seen that for n=10 P_S is about 61.19 nC/cm^2 whereas for n=18 it reduces to about 51.73 nC/cm^2.

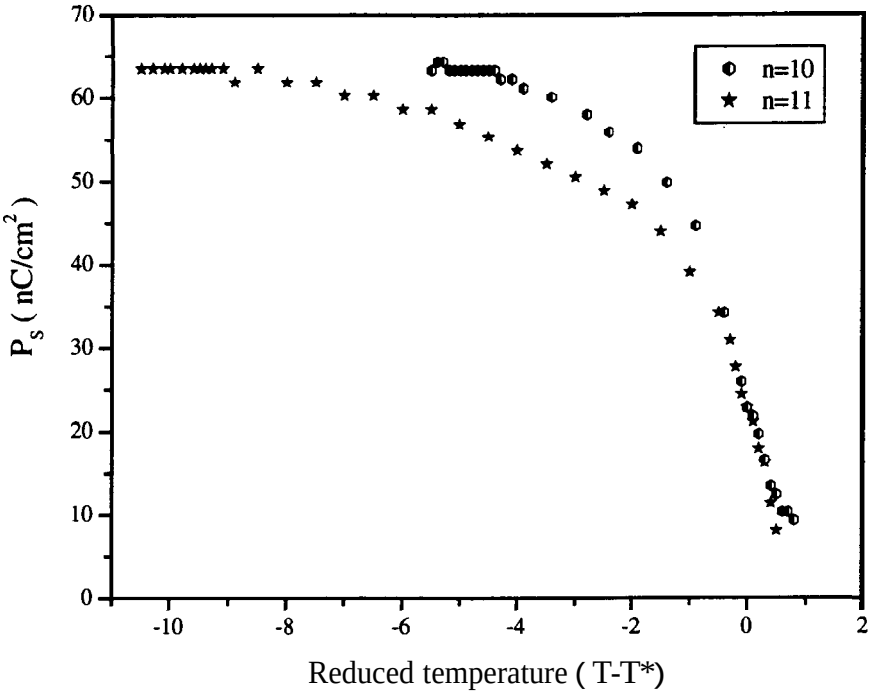

Fig 2.7 : Plot of spontaneous polarization *versus* reduced temperature for compounds 4 and 5 of the series 2.12.

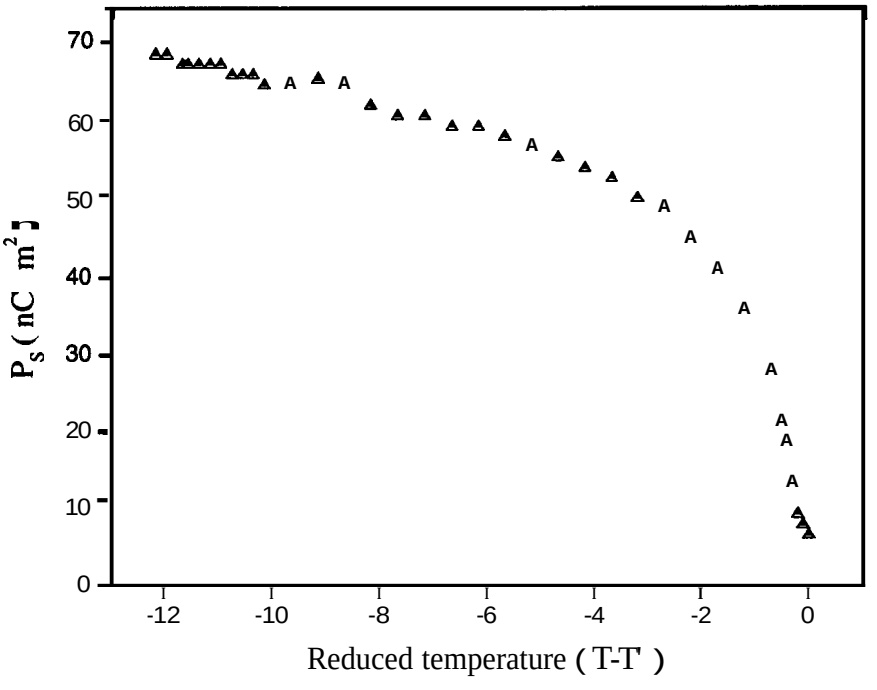

Fig 2.8 : Plot of spontaneous polarization *versus* reduced temperature for compound 6 of the series 2.12.

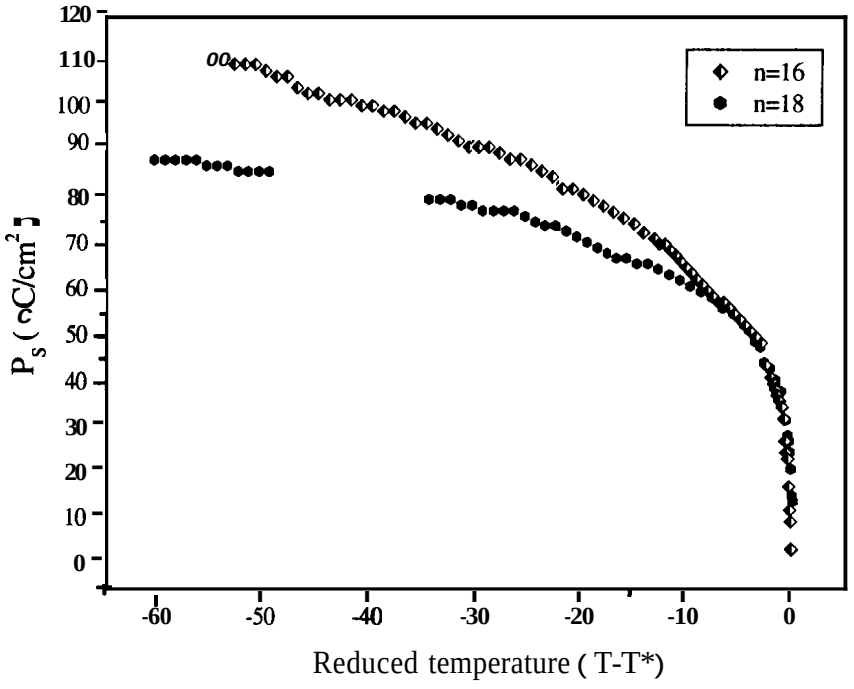

Fig 2.9 : Plot of spontaneous polarization versus reduced temperature for compounds 8 and 9 of the series 2.12.

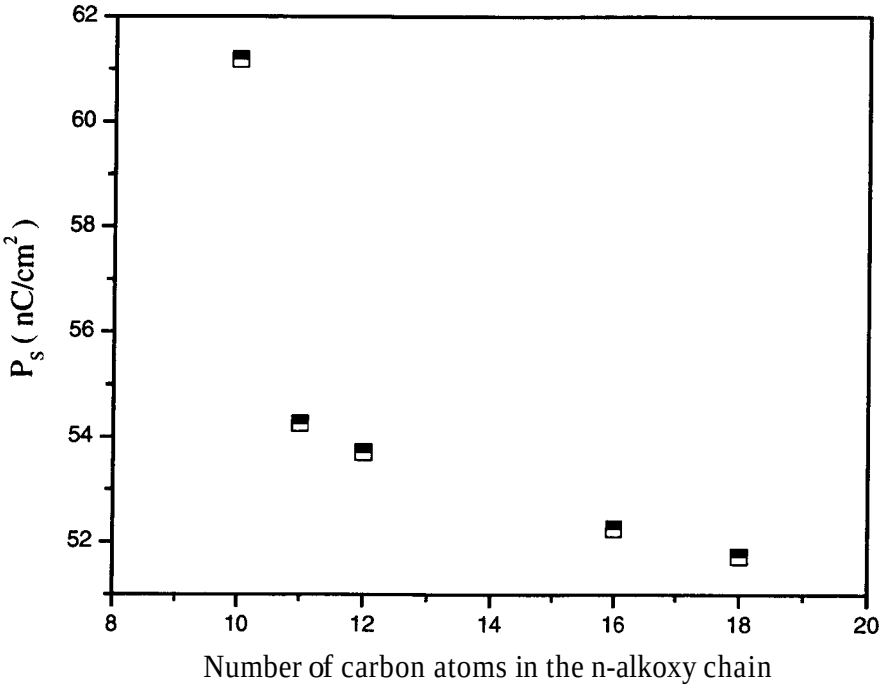

Fig 2.10 : Plot of the spontaneous polarization at $T-T^*$ = -4°C as a function of the n-alkoxy chain length.

2.2.2 Effect of the position of lateral fluoro substituent on the magnitude of spontaneous polarization in three phenyl ring esters:

The effect of polar lateral substituent on the magnitude of P_S can be explained in terms of:

(a) Proximity between the lateral polar group and the chiral center.

(b) The favourable orientation of the dipoles of the polar group and the chiral moiety.

It is believed that a polar group present close to the chiral center increases P_S due to the restricted internal rotation of the polar group by steric hindrance with the chiral group [47]. This is true in systems having ether as the linking group between the chiral moiety and the core. However, when the linking group is a carboxylate group, the increase or decrease in the magnitude of P_S due to the presence of a lateral polar substituent depends on the direction of orientation of the dipoles associated with the polar group and the chiral group. This is because, in the latter case since the chiral tail is conformationally correlated with the core less tightly than in the former case, the internal rotation of the polar group becomes more feasible and hence the dipoles can orient appropriately. An increase in the value of P_S is observed when the dipoles add up and a decrease in the value is seen when they cancel each other. The favourable orientation of the dipoles thereby either opposing each other or adding to each other in turn depends on the stable conformation the molecule would prefer to take so as to relieve the dipole-dipole interaction between the polar substituent and the group linking the core to the chiral moiety.

The results obtained from the polarization measurement carried out on the n-decyloxy homologue of the series **2.12** can be compared with those of the series **2.13** [25] and **2.14** [25]. Table **2.2** shows the maximum values of the P_S obtained for the n-decyloxy homologue of the three series:

Table : 2.2

Series number	P_S (nC/cm^2)
2.13	**-80**
2.14	≈100
2.12	≈64

From the table it is seen that for the series 2.14 which has a fluoro substituent *ortho* to the alkoxy chain there is a raise in the P_S value to 100 instead of 80 seen in case of series 2.13 which does not have any substituent. It is interesting to note that for the series 2.12, which has an additional lateral fluoro substituent close to the chiral center, the P_S value decreases to about 64 nC/cm^2. This decrease in the value of spontaneous polarization can be explained as follows:

In case of series 2.12 since the 1-methylheptyl group is remote from the core (separated by a carboxyl group), the lateral fluoro substituent close to the chiral center is free to orient itself so as to relieve the dipole-dipole interaction with the carbonyl group. Therefore the most stable conformation it would prefer to take is as shown in figure 2.11.

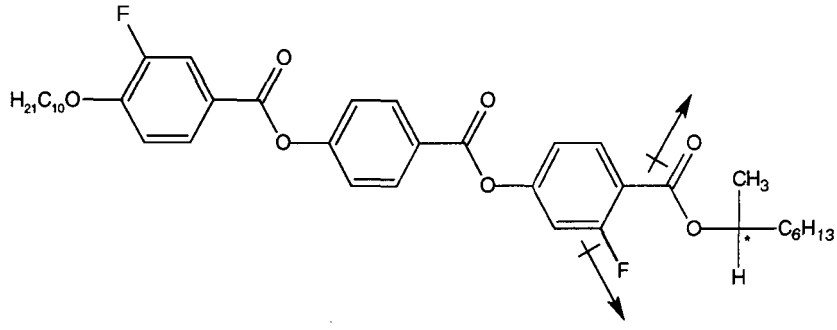

Fig 2.11

Thus, it is probable that in this stable conformation the dipole of the lateral fluoro substituent is opposing that of the carbonyl group thereby resulting in a decrease of the net lateral dipole and hence a decrease in the value of P_S.

2.3 Experimental:

4-Bromo-2-fluoroanisole, (2.17)

This was prepared following a procedure of Kelly [48]. Thus, bromine (12.7g, 69.85mmol) in anhydrous dichloromethane (20ml) was added dropwise during one hour to a solution of 2-fluoroanisole (8.81g, 69.85mmol) in anhydrous dichloromethane (50ml) at room temperature. The red colour disappeared immediately on addition and steady flow of HBr was observed. After the addition was complete the resultant solution was left overnight, poured into ice cold water and extracted with CH_2Cl_2. The combined organic solution was washed with 10% $NaHCO_3$ solution (2X25ml), water (3X25ml) and dried over Na_2SO_4. The solvent was removed from the filtered solution to give a crude product which was distilled under reduced pressure to yield pure 4-bromo-2-fluoroanisole (13.4g, 81.9%), b.p. 84°C/7mm (Reported [48] b.p. 98°C/20 mm).

4-Bromo-3-fluoroanisole, (2.18)

This was prepared following the above procedure using 3-fluoroanisole. Yield 71.7%, b.p. 68-70°C/1.5mm (Reported [48] b.p. 214-216°C at atm. pressure).

3-Fluoro-4-methoxybenzonitrile, (2.19)

This was prepared following a procedure of Kelly [48]. Thus, a solution of 4-bromo-2-fluoroanisole (50.1g, 244mmol), anhydrous cuprous cyanide (CuCN) (33g, 368.7mmol) and dry dimethylformamide (DMF, 300ml) was refluxed for twenty hours with stirring under anhydrous conditions. The cooled mixture was added to a solution of anhydrous ferric chloride ($FeCl_3$, 40g) and concentrated hydrochloric acid (15ml) in water (450ml) and stirred for 30 minutes at 50-60°C. The resultant mixture was extracted with ether (3X300ml), the combined ethereal extracts was washed with 5N hydrochloric acid (2X100ml), water (3X100ml), 5% ice cold NaOH (2X100ml), water (3X100ml) and dried over Na_2SO_4. The solvent was removed from the filtered solution to yield a residue, which was purified by column chromatography on silica

gel using chloroform:petroleum ether (75:25) mixture as eluent. The crude product was crystallized from benzene:petroleum ether mixture to yield pure 3-fluoro-4-methoxybenzonitrile (25.7g, 70%), m.p. 98.1-98.9°C (Reported [48] m.p. 98-99°C).

2-Fluoro-4-methoxybenzonitrile, (2.20)

This was prepared following the above procedure 4-bromo-3-fluoroanisole. Yield 77.5%, m.p. 59-60°C (Reported [48] m.p. 59-60°C).

3-Fluoro-4-hydroxybenzonitrile, (2.21)

This was prepared following a procedure of Kelly [48]. Thus, a homogeneous mixture of finely powdered 3-fluoro-4-methoxybenzonitrile (19g, 125.7mmol), crushed anhydrous aluminium chloride (33g, 251.4mmol), and sodium chloride (7.4g, 125.7mmol) was heated at a temperature of 190°C for one hour in a sublimation jacket. Analysis by TLC indicated complete absence of the starting material. The molten raw product was added carefully to ice cold hydrochloric acid and the resultant mixture was extracted with ether (3X100ml). The combined organic extracts was washed with water (3X100ml) and dried (Na_2SO_4). The solvent was removed from the filtered solution to yield a residue, which was purified by column chromatography on silica gel using 5% ethyl acetate in chloroform as eluent. The crude product was crystallized from toluene to yield 3-fluoro-4-hydroxybenzonitrile (14.5g, 84%), m.p.133.7-134 °C (Reported [48] m.p. 134-135 °C).

2-Fluoro-4-hydroxybenzonitrile, (2.22)

This was prepared following the above procedure 2-fluoro-4-methoxybenzonitrile. Yield 69%, m.p. 121-122°C (Reported [48] m.p. 117-118°C).

3-Fluoro-4-heptyloxybenzonitrile, (2.23)

A mixture of **3-fluoro-4-hydroxybenzonitrile** (4g, 29mmol), 1-bromoheptane (6.23g, 34.8mmol), anhydrous potassium carbonate (12g, 87 mmol), and butan-2-one

(75ml) was heated overnight under gentle reflux. Then the reaction mixture was allowed to come to room temperature and was poured into ice cold water. The organic layer was separated and the aqueous layer was extracted with ether (3X50ml). The combined organic extracts was washed with water (3X50ml), dilute hydrochloric acid (2X25ml), again with water (3X50ml) and dried over Na_2SO_4. The solvent was removed from the filtered solution to give a crude product which was distilled under reduced pressure to yield pure 3-fluoro-4-heptyloxybenzonitrile (6.6g, 96.2%), b.p. 120°C/1.5mm .

The physical data of the cognate preparations of the other 3-fluoro-4-n-alkoxybenzonitriles are given in table 2.3.

Table : 2.3

Compound number	n	Observed b.p.°C/mm or m.p °C
1	8	12010.7
2	9	140-14510.7
3	10	28.0-28.5
4	11	34.0-35.0
5	12	32.0-34.0
6	14	42.0-42.5

3-Fluoro-4-n-heptyloxybenzoicacid, (2.24)

A solution of **3-fluoro-4-heptyloxybenzonitrile** (6.2g, 26.4mmol), concentrated sulphuric acid (6.5ml), water (6.5ml) and glacial acetic acid (65ml) was refluxed overnight. The reaction mixture was allowed to come to room temperature and poured into ice cold water. The resultant precipitate was filtered off, washed several times with water until it was neutral to litmus and dried. This was recrystallized from ethanol to yield the pure acid (4.7g, 70.2%), m.p. 123.4°C (Reported [36] m.p. 124°C)

The physical data of the cognate preparations of the other **3-fluoro-4-n-alkoxybenzoic** acids are given in table 2.4.

Table : 2.4

Compound number	n	Observed m.p. (°C)	Reported m.p. (°C)	Reference
1	8	118.0	117.0	[36]
2	9	112.5	112.0	[36]
3	10	109.0	108.0	[36]
4	11	113.5	-	-
5	12	109.0	108.5	[36]
6	14	113.0	-	
7	16	114.5	-	-
8	18	116.0	114.0	[36]

2-Fluoro-4-hydroxybenzoic acid, (2.25)

A solution of 2-fluoro-4-hydroxybenzonitrile(20g, 145.8mmol), sodium hydroxide (34g), and water (300ml) was refluxed for sixty hours. The reaction mixture was cooled to room temperature and poured into ice cold hydrochloric acid. The resultant precipitate was filtered off, washed several times with water until it was neutral to litmus, and dried (Na_2SO_4). This was recrystallized from minimum quantity of water to yield the pure acid (12g, 57.6%), m.p. 202-204 °C (Reported [49] m.p. 204-205°C).

Ethyl 2-fluoro-4-hydroxybenzoate,(2.26)

A mixture of 2-fluoro-4-hydroxybenzoic acid (12g, 71.3mmol), ethanol (150ml), and concentrated sulphuric acid (2ml) was refluxed for twentyfour hours. Excess ethanol was distilled off on a water bath. The reaction mixture was cooled to room temperature and poured into ice cold water and extracted several times with ether. Then the combined ethereal extracts was washed with water (3X25ml), 10% $NaHCO_3$ (2X25ml), again with water (3X25ml) until neutral to litmus and dried (Na_2SO_4). The

solvent was removed from the filtered solution to yield a residue, which was purified by column chromatography on silica gel using 10% ethyl acetate in chloroform as the eluent. The crude product was crystallized from benzene to yield pure ethyl 2-fluoro-4-hydroxybenzoate(11.5g, 82.7%), m.p.131-131.5°C.

Ethyl 2-fluoro-4-benzyloxybenzoate,(2.27)

A mixture of ethyl 2-fluoro-4-hydroxybenzoate (11g, 56mmol), benzyl chloride (10g, 79mmol), anhydrous potassium carbonate (27g, 195mmol) and butan-2-one (150ml) was refluxed for twentyfour hours. Excess butan-2-one was distilled off. Then, the reaction mixture was cooled to room temperature and poured into ice and concentrated hydrochloric acid and was extracted with several portions of ether. The combined ethereal extracts was washed with water (3X30ml) and dried over Na_2SO_4. The solvent was removed from the filtered solution to yield a residue, which was purified by column chromatography on silica gel using chloroform as the eluent to yield pure ethyl 2-fluoro-4-benzyloxybenzoate(14.5g, 90.3%), b.p. 160°C/0.5-1mm.

2-Fluoro-4-benzyloxybenzoicacid, (2.28)

A mixture of ethyl 2-fluoro-4-benzyloxybenzoate (14.5g, 50mmol), potassium hydroxide (18g), ethanol (180ml), and water (15ml) was refluxed for twenty hours. Excess ethanol was distilled off on a water bath. Then, the reaction mixture was cooled to room temperature and poured into ice and hydrochloric acid. The resultant precipitate was filtered and washed several times with water until it was neutral to litmus and dried. This was recrystallized from ethanol:water mixture to yield pure 2-fluoro-4-hydroxybenzoicacid (12g, 91.7%), m.p.166-167°C.

[S]-[+]-1-Methylheptyl-2-fluoro-4-benzyloxybenzoate, (2.29)

This was prepared following an esterification procedure of Hassner and Alexanian [50]. Thus, a mixture of 2-fluoro-4-benzyloxybenzoic acid (2g, 8.0mmol), [S]-[+]-octan-2-01 (1.2g, 8.8mmol), 4-N,N'-dimethylaminopyridine (DMAP) (0.099g, 0.8mmol) and dry dichloromethane (20ml) was stirred for five minutes. To this

mixture was added N,N'-dicyclohexylcarbodiimide (DCC) (1.84g, 8.8mmol) and stirring continued overnight at room temperature. The precipitated N,N'-dicyclohexylurea was filtered off and the filtrate diluted with dichloromethane (50ml). The resultant solution was washed with 5% aqueous acetic acid (2X20ml), water (3X30ml) and dried over Na_2SO_4. The solvent was removed from the filtered solution to yield a residue which was purified by column chromatography on silica gel using chloroform:petroleum ether (60:40) as eluent to yield pure [S]-[+]-1-methylheptyl-2-fluoro-4-benzyloxybenzoate as a viscous liquid (2g, 71%); $[\alpha]_D^{25}$ = 28.4' (1mg/ml in $CHCl_3$; ν_{max} (neat): 2950, 1710, 1620, 1580, 1260, 1020 cm^{-1}; δ: 0.87-0.90 (6H, t, $2XCH_3$,), 1.29-1.74 (13H, m, $5XCH_2$, $1XCH_3$), 5.09 (2H, s, Ar$\underline{CH_2}$OAr), 5.12-5.16 (1H, m, COO-$\underline{CH}$-), 6.69-7.9 (8H, m, ArH).

[R]-[-]-1-Methylheptyl-2-fluoro-4-benzyloxybenzoate, (2.30)

This was prepared following a procedure similar to the one described above for compound 2.29 but using [R]-[-]-octan-2-ol. Yield, 71%; $[\alpha]_D^{25}$ = -28.4' (1mg/ml in $CHCl_3$); ν_{max} (neat): 2950, 1710, 1620, 1580, 1260, 1020 cm^{-1}; δ: 0.87-0.90 (6H, t, $2XCH_3$,), 1.29-1.74 (13H, m, $5XCH_2$, $1XCH_3$), 5.09 (2H, s, Ar$\underline{CH_2}$OAr), 5.12-5.16 (1H, m, COO-$\underline{CH}$-), 6.69-7.9 (8H, m, ArH).

[S]-[+]-1-Methylheptyl-2-fluoro-4-hydroxybenzoate, (2.31)

A mixture of [S]-[+]-1-methylheptyl-2-fluoro-4-benzyloxybenzoate (1.962g, 5.5mmol) dissolved in ethyl acetate (50ml) and 5% Pd-C catalyst (0.5g) was stirred in an atmosphere of hydrogen till the calculated quantity of hydrogen was absorbed. The reaction mixture was then filtered and removal of the solvent under reduced pressure yielded a viscous liquid (1.328g, 90.4%); $[\alpha]_D^{25} = 22.8^{\circ}$ (1mg/ml in $CHCl_3$); ν_{max} (neat): 3300, 2950, 1700, 1690, 1620, 1460, and 1280 cm^{-1}; δ: 0.85-0.98 (6H, t, $2XCH_3$,), 1.27-1.75 (13H, m, $5XCH_2$, $1XCH_3$), 5.09-5.16 (1H, m, COO-$\underline{CH}$-), 6.6-7.8 (4H, m, ArH).

[R]-[-]-1-Methylheptyl-2-fluoro-4-hydroxybenzoate, (2.32)

This was prepared following a procedure similar to the one described above (2.31) using [R]-[-]-1-methylheptyl-2-fluoro-4-benzyloxybenzoate. Yield, 91%; $[\alpha]_D^{25}$ = -22.8' (1mg/ml in $CHCl_3$); ν_{max} (neat): 3300, 2950, 1700, 1690, 1620, 1460, and 1280 cm^{-1}; 6: 0.85-0.98 (6H, t, $2XCH_3$,), 1.27-1.75 (13H, m, $5XCH_2$, $1XCH_3$), 5.09-5.16 (1H, m, COO-CH-), 6.6-7.8 (4H, m, ArH).

[S]-[+]-1-Methylheptyl-4-(4'-benzyloxybenzoyloxy)-2-fluorobenzoate, (2.33)

A mixture of 4-benzyloxybenzoic acid (1g, 4.4mmol), [S]-[+]-1-methylheptyl-2-fluoro-4-hydroxybenzoate (1.3g, 4.8mmol), DCC (1g, 4.8mmol), DMAP (0.054g, 0.4mmol) and dry dichloromethane was stirred overnight at room temperature. N,N'-Dicyclohexylurea formed was filtered off and the filtrate diluted with dichloromethane (50ml). The combined organic solution was washed with 5% aqueous acetic acid (2X20ml), water (3X50ml) and dried over Na_2SO_4. The solvent was removed from the filtered solution to yield a residue which was purified by column chromatography on silica gel using chloroform:petroleum ether (60:40) as eluent to yield pure [S]-[+]-1-methylheptyl-4-(4'-benzyloxybenzoyloxy)-2-fluorobenzoate as a white solid which was crystallized from ethanol (2.0g, 87.5%); m.p. 91.7'~;$[\alpha]_D^{25}$ = 22.8' (1mg/ml in $CHCl_3$); ν_{max} (nujol): 2900, 1720, 1700, 1600, 1460, 1280, 1240 and 1060 cm^{-1}; 6: 0.87-0.89 (6H, t, $2XCH_3$,), 1.23-1.77 (13H, m, $5XCH_2$, $1XCH_3$), 5.14-5.20 (3H, m, COO-CH- and $ArCH_2OAr$), 7.06-8.14 (12H, m, ArH).

[R]-[-]-1-Methylheptyl-4-(4'-benzyloxybenzoyloxy)-2-fluorobenzoate, (2.34)

This was prepared following a procedure similar to the one described above (2.33) using [R]-[-]-1-methylheptyl-2-fluoro-4-hydroxybenzoate. Yield, 87%; m.p. 91.7°C; $[\alpha]_D^{25}$ = -21.27° (1mg/ml in $CHCl_3$); ν_{max} (nujol): 2900, 1720, 1700, 1600, 1460, 1280, 1240 and 1060 cm^{-1}; 6: 0.87-0.89 (6H, t, $2XCH_3$,), 1.23-1.77 (13H, m, $5XCH_2$, $1XCH_3$), 5.14-5.20 (3H, m, COO-CH- and $ArCH_2OAr$), 7.06-8.14 (12H, m, ArH).

[S]-[+]-1-Methylheptyl-4-(4'-hydroxybenzoyloxy)-2-fluorobenzoate, (2.35)

Hydrogenolysis of compound 2.33 was carried out in ethylacetate solution as described for compound 2.31. The compound was purified by column chromatography on silica gel using chloroform:ethylacetate mixture as eluent. Yield 93.56%; m.p. 62-63°C; $[\alpha]_D^{25}$ = 32.14' (1mg/ml in $CHCl_3$); ν_{max} (nujol): 3350, 2900, 1700, 1610, 1590,1450,1280, 1250 and 1060 cm^{-1}; 6: 0.87-0.89 (6H, t, $2XCH_3$,), 1.3-1.74 (13H, m, $5XCH_2$, $1XCH_3$), 2.98 (1H, s, ArOH), 5.15-5.16 (1H, m, COO-CH-), 7.01-8.07 (8H, m, ArH).

[R]-[-]-1-Methylheptyl-4-(4'-hydroxybenzoyloxy)-2-fluorobenzoate, (2.36)

This was prepared following a procedure similar to the one described above (2.35) using compound 2.34. Yield 93%; m.p. 62-63°C; $[\alpha]_D^{25}$ = -30.8° (1mg/ml in $CHCl_3$); ν_{max} (nujol): 3350, 2900, 1700, 1610, 1590,1450,1280, 1250 and 1060 cm''; 6: 0.87-0.89 (6H, t, $2XCH_3$,), 1.3-1.74 (13H, m, $5XCH_2$, $1XCH_3$), 2.98 (1H, s, ArOH), 5.15-5.16 (1H, m, COO-CH-), 7.01-8.07 (8H, m, ArH).

[S]-[+]-1-Methylheptyl-4-[4'-(3"-fluoro-4"-n-heptyloxybenzoyloxy)benzoyloxy]-2- fluorobenzoate

This was prepared following a procedure described for compound 2.29 using phenol 2.35 and 3-fluoro-4-n-heptyloxybenzoic acid. Yield, 73.5%; m.p. 63.0°C; $[\alpha]_D^{25}$ = 28' (1mg/ml in $CHCl_3$); ν_{max} (nujol): 2950, 1730, 1720, 1710, 1610, 1460, 1280, 1240 and 1050 cm^{-1}; 6: 0.86-0.93 (6H, t, $2XCH_3$), 1.27-1.9 (21H, m, $1XCH_3$, $9XCH_2$), 1.83-1.9 (2H, m, -$CH(CH_3)$-CH_2-), 4.11-4.14 (2H, t, -Ar-OCH_2-), 5.15-5.2 (1H, m, -COOCH-), 7.0-8.27 (10H, m, ArH).

The physical data of the cognate preparations of the other [S]-[+]-1-methylheptyl-4-[4'-(3"-fluoro-4"-n-alkoxybenzoyloxy)benzoyloxy]-2-fluorobenzoates are given below.

[S]-[+]-1-Methylheptyl-4-[4'-(3"-fluoro-4"-n-octyloxybenzoyloxy)benzoyloxy]-2-fluorobenzoate

Yield, 73%; m.p. 69.5°C; $[\alpha]_D^{25}$ = 29.4' (lmglml in $CHCl_3$); ν_{max} (nujol): 2950, 1730, 1720, 1710, 1610, 1460, 1280, 1240 and 1050 cm^{-1}; 6: 0.86-0.93 (6H, t, $2XCH_3$), 1.27-1.9 (23H, m, $1XCH_3$, $10XCH_2$), 1.83-1.9 (2H, m, -CH(CH_3)-$\underline{CH_2}$-), 4.11-4.14 (2H, t, -Ar-O$\underline{CH_2}$-), 5.15-5.2 (1H, m, -COO$\underline{CH}$-), 7.0-8.27 (10H, m, ArH).

[S]-[+]-1-Methylheptyl-4-[4'-(3"-fluoro-4"-n-nonyloxybenzoyloxy)benzoyloxy]-2-fluorobenzoate

Yield, 72.1%; m.p. 93.5°C; $[\alpha]_D^{25}$ = 26' (lmglml in $CHCl_3$); ν_{max} (nujol): 2950, 1730, 1720, 1710, 1610, 1460, 1280, 1240 and 1050 cm^{-1}; 6: 0.86-0.93 (6H, t, $2XCH_3$), 1.27-1.9 (25H, m, $1XCH_3$, $11XCH_2$), 1.83-1.9 (2H, m, -CH(CH_3)-$\underline{CH_2}$-), 4.11-4.14 (2H, t, -Ar-O$\underline{CH_2}$-), 5.15-5.2 (1H, m, -COO$\underline{CH}$-), 7.0-8.27 (10H, m, ArH).

[S]-[+]-1-Methylheptyl-4-[4'-(3"-fluoro-4"-n-decyloxybenzoyloxy)benzoyloxy]-2-fluorobenzoate

Yield, 77%; m.p. 101.0°C; $[\alpha]_D^{25}$ = 20° (1mg/ml in $CHCl_3$); ν_{max} (nujol): 2950, 1730, 1720, 1710, 1610, 1460, 1280, 1240 and 1050 cm^{-1}; 6: 0.86-0.93 (6H, t, $2XCH_3$), 1.27-1.9 (27H, m, $1XCH_3$, $12XCH_2$), 1.83-1.9 (2H, m, -CH(CH_3)-$\underline{CH_2}$-), 4.11-4.14 (2H, t, -Ar-O$\underline{CH_2}$-), 5.15-5.2 (1H, m, -COO$\underline{CH}$-), 7.0-8.27 (10H, m, ArH).

[S]-[+]-1-Methylheptyl-4-[4'-(3"-fluoro-4"-n-undecyloxybenzoyloxy)benzoyloxy]-2-fluorobenzoate

Yield, 75%; m.p. 90.0°C; $[\alpha]_D^{25}$ = 22° (1mg/ml in $CHCl_3$); ν_{max} (nujol): 2950, 1730, 1720, 1710, 1610, 1460, 1280, 1240 and 1050 cm^{-1}; 6: 0.86-0.93 (6H, t, $2XCH_3$), 1.27-1.9 (29H, m, $1XCH_3$, $13XCH_2$), 1.83-1.9 (2H, m, -CH(CH_3)-$\underline{CH_2}$-), 4.11-4.14 (2H, t, -Ar-O$\underline{CH_2}$-), 5.15-5.2 (1H, m, -COO$\underline{CH}$-), 7.0-8.27 (10H, m, ArH).

[S]-[+]-1-Methylheptyl-4-[4'-(3"-fluoro-4"-n-dodecyloxybenzoyloxy)benzoyloxy]- 2- fluorobenzoate

Yield, 76.5%; m.p. 60.5'~; $[\alpha]_D^{25}$ = 18' (1mg/ml in $CHCl_3$); ν_{max} (nujol): 2950, 1730, 1720, 1710, 1610, 1460, 1280, 1240 and 1050 cm^{-1}; 6: 0.86-0.93 (6H, t, $2XCH_3$), 1.27-1.9 (31H, m, $1XCH_3$, $14XCH_2$), 1.83-1.9 (2H, m, -CH(CH_3)-$\underline{CH_2}$-), 4.11-4.14 (2H, t, -Ar-O$\underline{CH_2}$-), 5.15-5.2 (1H, m, -COO$\underline{CH}$-), 7.0-8.27 (10H, m, ArH).

[S]-[+]-1-Methylheptyl-4-[4'-(3"-fluoro-4"-n-tetradecyloxybenzoyloxy) benzoyloxy] -2- fluorobenzoate

Yield, 78%; m.p. 57.0°C; $[\alpha]_D^{25}$ = 17.24° (1mg/ml in $CHCl_3$); ν_{max} (nujol): 2950, 1730, 1720, 1710, 1610, 1460, 1280, 1240 and 1050 cm^{-1}; 6: 0.86-0.93 (6H, t, $2XCH_3$), 1.27-1.9 (35H, m, $1XCH_3$, $16XCH_2$), 1.83-1.9 (2H, m, -CH(CH_3)-$\underline{CH_2}$-), 4.11-4.14 (2H, t, -Ar-$\underline{OCH_2}$-), 5.15-5.2 (1H, m, -COO$\underline{CH}$-), 7.0-8.27 (10H, m, ArH).

[S]-[+]-1-Methylheptyl-4-[4'-(3"-fluoro-4"-n-hexadecyloxybenzoyloxy) **benzoyloxy]-2-** fluorobenzoate

Yield, 81.7%; m.p. 62.0°C; $[\alpha]_D^{25}$ = 16.39° (1mg/ml in $CHCl_3$); v, (nujol): 2950, 1730, 1720, 1710, 1610, 1460, 1280, 1240 and 1050 cm^{-1}; 6: 0.86-0.93 (6H, t, $2XCH_3$), 1.27-1.9 (39H, m, $1XCH_3$, $18XCH_2$), 1.83-1.9 (2H, m, -CH(CH_3)-$\underline{CH_2}$-), 4.11-4.14 (2H, t, -Ar-$\underline{OCH_2}$-), 5.15-5.2 (1H, m, -COO$\underline{CH}$-), 7.0-8.27 (10H, m, ArH).

[S]-[+]-1-Methylheptyl-4-[4'-(3"-fluoro-4"-n-octadecyloxybenzoyloxy) **benzoyloxy]-2-** fluorobenzoate

Yield, 82%; m.p. 52.0°C; $[\alpha]_D^{25}$ = 19.35° (1mg/ml in $CHCl_3$); ν_{max} (nujol): 2950, 1730, 1720, 1710, 1610, 1460, 1280, 1240 and 1050 cm^{-1}; 6: 0.86-0.93 (6H, t, $2XCH_3$), 1.27-1.9 (43H, m, $1XCH_3$, $20XCH_2$), 1.83-1.9 (2H, m, -CH(CH_3)-$\underline{CH_2}$-),

4.11-4.14 (2H, t, -Ar-$\underline{OCH_2}$-), 5.15-5.2 (1H, m, -COO$\underline{CH}$-), 7.0-8.27 (10H, m, ArH).

[R]-[-]-1-Methylheptyl-4-[4'-(3"-fluoro-4"-n-octyloxybenzoyloxy)benzoyloxy]-2-fluorobenzoate

Yield, 74%; m.p.70.0°C; $[\alpha]_D^{25}$ = -29.4' (1mg/ml in $CHCl_3$); ν_{max} (nujol): 2950, 1730, 1720, 1710, 1610, 1460, 1280, 1240 and 1050 cm^{-1}; 6: 0.86-0.93 (6H, t, $2XCH_3$), 1.27-1.9 (23H, m, $1XCH_3$, $10XCH_2$), 1.83-1.9 (2H, m, -CH(CH_3)-$\underline{CH_2}$-), 4.11-4.14 (2H, t, -Ar-$\underline{OCH_2}$-), 5.15-5.2 (1H, m, -COO$\underline{CH}$-), 7.0-8.27 (10H, m, ArH).

REFERENCES

[1] G.W.Gray, Molecular Structure and the Properties of Liquid Crystals, Academic Press, New York (1962).

[2] R.B.Meyer, L.Liebert, L.Strzelecki and P.Keller, J. de Phys. Lett., 36, L69 (1975).

[3] N.A.Clark and S.T.Lagerwall, Appl. Phys. Lett., 36, 899 (1969).

[4] A.D.L.Chandani, E.Gorecka, Y.Ouchi, H.Takezoe and A.Fukuda, Jpn. J. Appl. Phys., 28, L1265 (1989).

[5] N.Yamamoto, Y.Yamada, N.Koshobu, K.Mori, K.Nakamda, H.Orihara, Y.Ishibashi, Y.Suzuki and I.Kawamura, Jpn. J. Appl. Phys., 31, 3186 (1992).

[6] T.Moriyama, J.Kajita, Y.Takanishi, K.Ishikawa, H.Takezoe and A.Fukuda, Jpn. J. Appl. Phys., 32,589 (1993).

[7] T.Orama, T.Masuda, S.Hamada, S.Takahashi, S.Kurita, I.Kawamura and T.Hagiwara, Jpn. J. Appl. Phys., 32, L668 (1993).

[8] A.D.L.Chandani, T.Hagiwara, Y.Suzuki, Y.Ouchi, H.Takezoe and A.Fukuda, J. Appl. Phys., 27, L729 (1988).

[9] H.Takezoe, J.Lee, A.D.L.Chandani, E.Gorecka, Y.Ouchi, A.Fukuda, K.Terashima and K.Furukawa, Ferroelectrics, 114,187 (1991).

[10] H.Takezoe, A.D.L.Chandani, E.Gorecka, Y.Ouchi, A.Fukuda, K.Terashima and A.Kishi, Abs. *2'''*. Int. Symp. on FLCS., Goteborg, p. 026 (1989).

[11] H.Takezoe, A.D.L.Chandani, J.Lee, E.Gorecka, Y.Ouchi and A.Fukuda, Abs. *2'''*. Int. Symp. on *FLCs.*, Goteborg, p. P108 (1989).

[12] Y.Yamada, N.Yamamoto, K.Mori, K.Nakamura, T.Hagiwara, Y.Suzuki, I.Kawamura, H.Orihara and Y.Ishibashi, Jpn. J. Appl. Phys., 29, 1757 (1990).

[13] H.Moritake, A.Ozaki and K.Yoshino, Jpn. J. Appl. Phys., 30,2373 (1991).

[14] A.Fukuda, Y.Takanishi, T.Ishikawa and H.Takezoe, J. *Mater.* Chem., 4, 997 (1994).

[15] J.W.Goodby, A.J.Slaney, I.Nishiyama, J.D.Vuijk, P.Styring and K.J.Toyne, Mol. *Cryst.* Liq. *Cryst.*, 243, 231 (1994).

[16] S.T.Lagerwall, Ferroelectric and Antiferroelectric Liquid Crystals, Wiley-VCH, Toronto (1999).

[17] Y.Takanishi, K.Hiraoka, V.K.Agrawal, H.Takezoe, A.Fukuda and M.Matsushita, Jpn. J. Appl. Phys., 30, 2030 (1991).

[18] J.W.Goodby, J. Mater. Chem., 1,307 (1991).

[19] A.J.Slaney and J.W.Goodby, J. Mater. Chem., 1, 5 (1991).

[20] J.W. Goodby, J.S.Patel and E.Chin., J. Mater. Chem., 2, 197 (1992).

[21] I.Nishiyama and J.W.Goodby, J. Mater. Chem., 3, 149 (1993).

[22] J.W.Goodby, I.Nishiyama, A.J.Slaney, C.S.Booth and K.J.Toyne, *Liq. Cryst.*, **14**, 37 (1993).

[23] K.Furukawa, K.Terashima, M.Ichihashi, S.Saitoh, K.Miyazawa and T.Inukai, Ferroelectrics, **85**, 451 (1988).

[24] M.E.Neubert, S.S.Keast, M.C.Ezenyilimba, C.A.Hanlon and W.C.Jones, Mol. *Cryst. Liq. Cryst.*, 237, 193 (1993).

[25] V.Faye, J.C.Rouillon, C.Destrade and H.T.Nguyen, *Liq.Cryst.*, **19**, 47 (1995).

[26] G.Heppke, J.M.Hollidt, D.Moro, D.Lotzsch, R.P.Tuffin and J.W.Goodby, 15'' Int. *Liq. Cryst. Conf.*, Budapest, Abst. J-Sbp9 (1994).

[27] N.Kasturaiah, B.K.Sadashiva, S.Krishnaprasad and G.G.Nair, *Liq. Cryst.*, 24, 639 (1998).

[28] S.Inui, S.Kawano, M.Saito, H.Iwane, Y.Takanishi, K.Haroaka, Y.Ouchi, H.Takezoe and A.Fukuda, Jpn. J. Appl. Phys., 29, L987 (1990).

[29] I.Nishiyama, A.Yoshizawa, M.Fukumasa and T.Hirai, Jpn. J. Appl. Phys., 28, L2248 (1989).

[30] Y.Suzuki, T.Hagiwara and I.Kawamura, *Liq. Cryst.*, 6, 167 (1989).

[31] J.W.Goodby, A.J.Slaney, C.J.Booth, I.Nishiyama, J.D.Vuijk, P.Styring and K.J.Toyne, Mol. *Cryst. Liq. Cryst.*, 243, 231 (1994).

[32] S.Takehara, T.Shoji, M.Osawa, H.Ogawa and T.Fujisawa, *12th* Jpn. Symp. *Liq. Cryst.*, Nagoya, Abst. 2F18 (1986).

[33] A.J.Seed, M.Hird, P.Styring, H.F. Gleeson and J.T.Mills, Mol. *Cryst. Liq. Cryst.*, 299, 19 (1997).

[34] A.J.Seed, M.Hird, P.Styring, H.F. Gleeson and J.T.Mills, Unpublished results (1996).

[35] J.W.O'Sullivan, Y.P.Panarin, J.K.Vij, A.J.Seed, M.Hird and J.W.Goodby, J. Phys. *Conden.* Matter., 8, L551 (1996).

[36] G.W.Gray and B.Jones, J. Chem. *Soc.*, 2556 (1954).

[37] P.Cluzeau, H.T.Nguyen, C.Destrade, N.Isaert, P.Barois and A.Babeau, Mol. *Cryst.* Liq. *Cryst.*, **260**, 69 (1995)

[38] H.T.Nguyen, J.C.Rouillon, P.Cluzeau, G.Sigaud, C.Destrade and N.Isaert, Liq. *Cryst.*, 17,571 (1994).

[39] E.Chin, J.W.Goodby, J.M.Geary, J.S.Patel and T.M.Leslie, Mol. *Cryst.* Liq. *Cryst.*, 146, 325 (1987).

[40] J.W.Goodby, E.Chin, J.M.Geary, J.S.Patel and P.L.Finn, J. Chem. *Soc.* Faraday Trans. I., 83,3429 (1987).

[41] B.I.Ostrovskii, A.Z.Rabinovich, A.S.Sonin, A.Strukov and N.I.Chernova, J.E.T.P. Lett., 25, 70 (1977).

[42] L.J.Yu, H.Lee, C.S.Bak and M.M.Labes, Phys. Rev. Lett., 36,388 (1976).

[43] S.S.Bawa, A.M.Biradar, K.Saxena and Subhas Chandra, Rev. *Sci.* Instrum., 59, 2023 (1988).

[44] C.B.Sawyer and C.H.Tower, Phys. Rev., 35,369 (1930).

[45] F. Jona and G.Shirane, Ferroelectric Crystals, Pergamon Press, New York (1992).

[46] H.Diamant, K.Drenck and R.Pepinsky, Rev. Sci. Instrum., 28, 30 (1957).

[47] K.Furukawa, K.Terashima, M.Ichihashi, S.Saitoh, K.Miyazawa and T.Inukai, Ferroelectrics, **85**, 451 (1988).

[48] S.M.Kelly, Helv. Chim. *Acta.*, 67, 1572 (1984).

[49] G.W.Gray, C.Hogg and D.Lacey, Mol. *Cryst.* Liq. *Cryst.*, 67, 1 (1981).

[50] A.Hassner and V.Alexanian, Tetrahedron Lett., 4475 (1978).